EUROPEAN ORGANIZATION FOR NUCLEAR RESEARCH (CERN)

CERN-PH-EP/2015-297
2016/04/14

CMS-EXO-12-054

Search for dark matter and unparticles produced in association with a Z boson in proton-proton collisions at $\sqrt{s} = 8\,\text{TeV}$

The CMS Collaboration*

Abstract

A search for evidence of particle dark matter (DM) and unparticle production at the LHC has been performed using events containing two charged leptons, consistent with the decay of a Z boson, and large missing transverse momentum. This study is based on data collected with the CMS detector corresponding to an integrated luminosity of 19.7 fb^{-1} of pp collisions at the LHC at a center-of-mass energy of 8 TeV. No significant excess of events is observed above the number expected from the standard model contributions. The results are interpreted in terms of 90% confidence level limits on the DM-nucleon scattering cross section, as a function of the DM particle mass, for both spin-dependent and spin-independent scenarios. Limits are set on the effective cutoff scale Λ, and on the annihilation rate for DM particles, assuming that their branching fraction to quarks is 100%. Additionally, the most stringent 95% confidence level limits to date on the unparticle model parameters are obtained.

Published in Physical Review D as doi:10.1103/PhysRevD.93.052011.

*See Appendix A for the list of collaboration members

1 Introduction

Ample evidence from astrophysical measurements supports the existence of dark matter (DM), which is assumed to be responsible for galactic gravitation that cannot be attributed to baryonic matter [1–3]. Recent DM searches have exploited a number of methods including direct detection [4–11], indirect detection [12, 13], and particle production at colliders [14–26]. The currently favored possibility is that DM may take the form of weakly interacting massive particles. The study presented here considers a mechanism for producing such particles at the CERN LHC [27]. In this scenario, a Z boson, produced in pp collisions, recoils against a pair of DM particles, $\chi\overline{\chi}$. The Z boson subsequently decays into two charged leptons ($\ell^+\ell^-$, where $\ell =$ e or μ) producing a clean dilepton signature together with missing transverse momentum due to the undetected DM particles. In this analysis, the DM particle χ is assumed to be a Dirac fermion or a complex scalar particle of which the coupling to standard model (SM) quarks q can be described by one of the effective interaction terms [28]:

$$\text{Vector, spin independent(D5)}: \quad \frac{\bar{\chi}\gamma^{\mu}\chi\bar{q}\gamma_{\mu}q}{\Lambda^2};$$

$$\text{Axial vector, spin dependent(D8)}: \quad \frac{\bar{\chi}\gamma^{\mu}\gamma^{5}\chi\bar{q}\gamma_{\mu}\gamma^{5}q}{\Lambda^2};$$

$$\text{Tensor, spin dependent(D9)}: \quad \frac{\bar{\chi}\sigma^{\mu\nu}\chi\bar{q}\sigma_{\mu\nu}q}{\Lambda^2};$$

$$\text{Vector, spin independent(C3)}: \quad \frac{\chi^{\dagger}\overleftrightarrow{\partial}_{\mu}\chi\bar{q}\gamma^{\mu}q}{\Lambda^2};$$

where Λ parametrizes the effective cutoff scale for interactions between DM particles and quarks. The operators denoted by D5, D8, and D9 couple to Dirac fermions, while C3 couples to complex scalars. The corresponding Feynman diagrams for production of a DM pair with a Z boson and up to one jet are shown in Fig. 1. A search similar to the one presented here has been performed by the ATLAS Collaboration [26], where the DM particle is assumed to be a Dirac fermion and couples to either vector bosons or quarks.

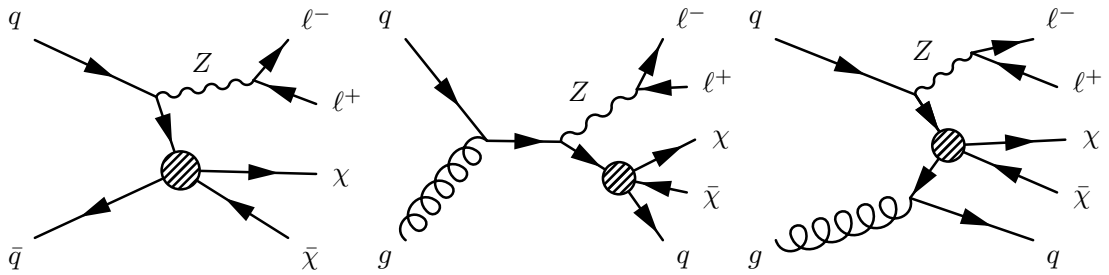

Figure 1: The principal Feynman diagrams for the production of DM pairs in association with a Z boson. In the middle and right-hand diagrams an additional quark is produced. The hatched circles indicate the interaction modeled with an effective field theory.

The unparticle physics concept [29–32] is particularly interesting because it is based on scale invariance, which is anticipated in many beyond-the-SM physics scenarios [33–35]. The unparticle stuff of the scale-invariant sector appears as a noninteger number of invisible massless particles. In this scenario, the SM is extended by introducing a scale-invariant Banks-Zaks ($\mathcal{BZ}$) field, which has a nontrivial infrared fixed point [36]. This field can interact with SM particles by exchanging heavy particles with a high mass scale $M_{\mathcal{U}}$. Below this mass scale, the coupling is nonrenormalizable and the interaction is suppressed by powers of $M_{\mathcal{U}}$. The interaction Lagrangian density can be expressed as $\mathcal{L}_{\text{int}} = \mathcal{O}_{\text{SM}}\mathcal{O}_{\mathcal{BZ}}/M_{\mathcal{U}}^{k}$, where $\mathcal{O}_{\text{SM}}$ is the operator for the

SM field with scaling dimension d_{SM}, $\mathcal{O}_{\mathcal{BZ}}$ is the operator for the $\mathcal{BZ}$ field with scaling dimension $d_{\mathcal{BZ}}$, and $k = d_{\mathrm{SM}} + d_{\mathcal{BZ}} - 4 > 0$. At an energy scale of $\Lambda_{\mathcal{U}}$, dimensional transmutation is induced by renormalization effects in the scale-invariant $\mathcal{BZ}$ sector, and $\mathcal{O}_{\mathcal{BZ}}$ can be matched to a new set of operators below $\Lambda_{\mathcal{U}}$ with the interaction form

$$\mathcal{L}_{\mathrm{int}}^{\mathrm{eff}} = C_{\mathcal{U}} \frac{\Lambda_{\mathcal{U}}^{d_{\mathcal{BZ}} - d_{\mathcal{U}}}}{M_{\mathcal{U}}^{k}} \mathcal{O}_{\mathrm{SM}} \mathcal{O}_{\mathcal{U}} = \frac{\lambda}{\Lambda_{\mathcal{U}}^{d_{\mathcal{U}}}} \mathcal{O}_{\mathrm{SM}} \mathcal{O}_{\mathcal{U}}, \tag{1}$$

in which $C_{\mathcal{U}}$ is a normalization factor fixed by the matching, $d_{\mathcal{U}}$ represents the possible noninteger scaling dimension of the unparticle operator $\mathcal{O}_{\mathcal{U}}$, and the parameter $\lambda = C_{\mathcal{U}} \Lambda_{\mathcal{U}}^{d_{\mathcal{BZ}}} / M_{\mathcal{U}}^{k}$ is a measure of the coupling between SM particles and unparticles. In general, an unparticle does not have a fixed invariant mass but has instead a continuous mass spectrum, and its real production in low energy processes described by the effective field theory in Eq. (1) can give rise to an excess of missing energy because of the possible nonintegral values of the scaling dimension $d_{\mathcal{U}}$. In the past, the reinterpretation [37] of LEP single-photon data has been used to set unparticle limits. A recent search for unparticles at CMS [14] in monojet final states has shown no evidence for their existence. In this paper, a scalar unparticle with real emission is considered, and the scaling dimension $d_{\mathcal{U}} > 1$ is constrained by the unitarity condition. Figure 2 shows the two tree-level diagrams considered in this paper for the production of unparticles associated with a Z boson.

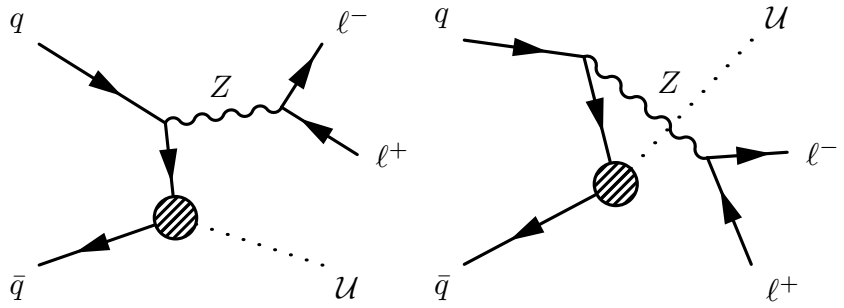

Figure 2: Feynman diagrams for unparticle production in association with a Z boson. The hatched circles indicate the interaction modeled with an effective field theory.

Both the DM and unparticle scenarios considered in this analysis produce a dilepton (e^+e^- or $\mu^+\mu^-$) signature consistent with a Z boson, together with a large magnitude of missing transverse momentum. The analysis is based on the full data set recorded by the CMS detector in 2012, which corresponds to an integrated luminosity of $19.7 \pm 0.5\,\mathrm{fb}^{-1}$ [38] at a center-of-mass energy of 8 TeV.

2 CMS detector

The CMS detector is a multipurpose apparatus well suited to study high transverse momentum (p_{T}) physics processes in pp collisions. The central feature of the CMS apparatus is a superconducting solenoid of 6 m internal diameter, providing a magnetic field of 3.8 T. Within the superconducting solenoid volume are a silicon pixel and strip tracker, a lead tungstate crystal electromagnetic calorimeter (ECAL), and a brass and scintillator hadron calorimeter (HCAL), each composed of a barrel and two end cap sections. Forward calorimeters extend the pseudorapidity [39] coverage provided by the barrel and end cap detectors. The electromagnetic calorimeter consists of 75 848 lead tungstate crystals, which provide coverage in pseudorapidity $|\eta| < 1.479$ in a barrel region and $1.48 < |\eta| < 3.00$ in two end cap regions (EE). A

preshower detector consisting of two planes of silicon sensors interleaved with a total of $3X_0$ of lead is located in front of the EE. The electron momentum is estimated by combining the energy measurement in the ECAL with the momentum measurement in the tracker. The momentum resolution for electrons with $p_T \approx 45\,\text{GeV}$ from $Z \to ee$ decays ranges from 1.7% for nonshowering electrons in the barrel region to 4.5% for showering electrons in the end caps [40]. Muons are measured in the pseudorapidity range $|\eta| < 2.4$, with gas-ionization detectors embedded in the steel flux-return yoke outside the solenoid. The muon detection planes are made using three technologies: drift tubes, cathode strip chambers, and resistive plate chambers. Matching muons to tracks measured in the silicon tracker results in a relative transverse momentum resolution for muons with $20 < p_T < 100\,\text{GeV}$ of 1.3–2.0% in the barrel and better than 6% in the end caps. The p_T resolution in the barrel is better than 10% for muons with p_T up to 1 TeV [41]. The first level of the CMS trigger system, composed of custom hardware processors, uses information from the calorimeters and muon detectors to select the most interesting events, in a fixed time interval of less than $4\,\mu$s. The high-level trigger processor farm further decreases the event rate from around 100 kHz to less than 1 kHz, before data storage. A more detailed description of the CMS detector, together with a definition of the coordinate system used and the relevant kinematic variables, can be found in Ref. [39]. Variables of particular relevance to the present analysis are the missing transverse momentum vector $\vec{p}_T^{\,\text{miss}}$ and the magnitude of this quantity, E_T^{miss}. The quantity $\vec{p}_T^{\,\text{miss}}$ is defined as the projection on the plane perpendicular to the beams of the negative vector sum of the momenta of all reconstructed particles in an event.

3 Simulation

Samples of simulated DM particle events are generated using MADGRAPH 5.2.1 [42] matched to PYTHIA 6.4.26 [43] using tune Z2* for parton showering and hadronization. The PYTHIA 6 Z2* tune uses the CTEQ6L [44] parton distribution set. This tune is derived from the Z1 tune [45], which is based on CTEQ5L. The effective cutoff scale Λ is set to 1 TeV. The events for the unparticle models are generated with PYTHIA 8.1 [46–48] assuming a renormalization scale $\Lambda_{\mathcal{U}} = 15\,\text{TeV}$, using tune 4C [49] for parton showering and hadronization. We evaluate other values of $\Lambda_{\mathcal{U}}$ by rescaling the cross sections as needed. The parameter $\Lambda_{\mathcal{U}}$ acts solely as a scaling factor for the cross section and does not influence the kinematic distributions of unparticle production [48]. Figure 3 shows the distribution of E_T^{miss} at the generator level for both DM and unparticle production. In the unparticle scenario, the events with larger scaling dimension $d_{\mathcal{U}}$ tend to have a broader E_T^{miss} distribution. For DM production, the shape of the E_T^{miss} is similar for couplings D5, D8, and C3, where the vector or axial vector couplings tend to produce nearly back-to-back DM particles. This configuration is less strongly favored for the tensor couplings, and thus the D9 couplings show a much broader E_T^{miss} distribution.

The POWHEG 2.0 [50–54] event generator is used to produce samples of events for the $\mathrm{t\bar{t}}$ and tW background processes. The ZZ, WZ, and Drell–Yan (DY, $Z/\gamma^* \to \ell^+\ell^-$) processes are generated using the MADGRAPH 5.1.3 [55] event generator. The default set of parton distribution functions (PDFs) CTEQ6L [56] is used for generators that are leading order (LO) in α_s, while the CT10 [57] set is used for next-to-leading-order (NLO) generators. The NLO calculations are used for background cross sections, whereas only LO calculations are available for the signal processes. For all Monte Carlo (MC) samples, the detector response is simulated using a detailed description of the CMS detector, based on the GEANT4 package [58]. Minimum bias events are superimposed on the simulated events to emulate the additional pp interactions per bunch crossing (pileup). All MC samples are corrected to reproduce the pileup distribution as measured in the data. The average number of pileup events per proton bunch crossing is about

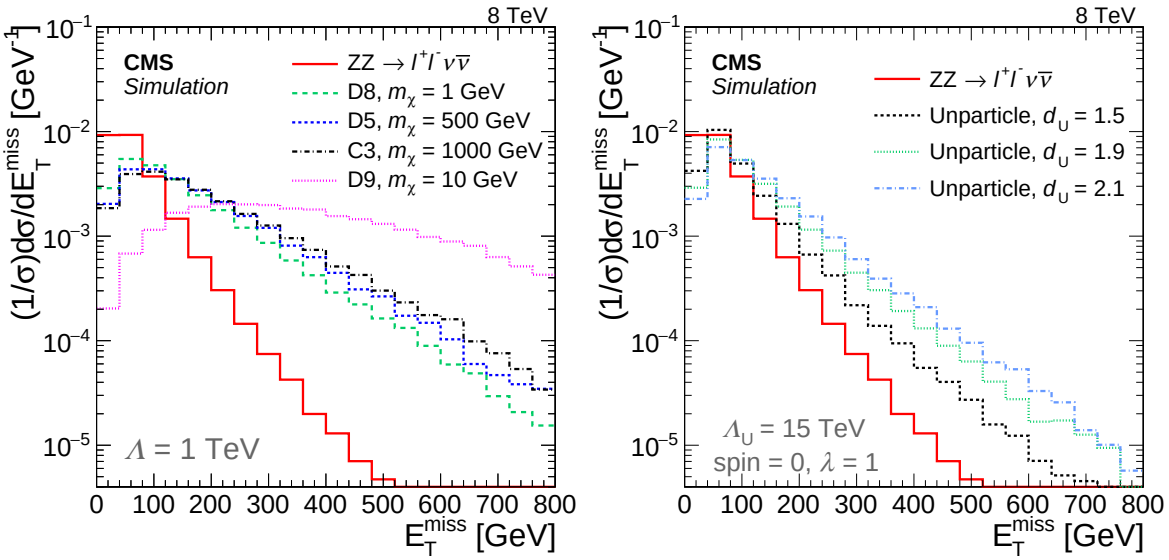

Figure 3: The distribution in $E_{\mathrm{T}}^{\mathrm{miss}}$ at the generator level, for DM (left) and unparticle (right) scenarios. The DM curves are shown for different m_{χ} with vector (D5), axial-vector (D8), and tensor (D9) coupling for Dirac fermions, and vector (C3) coupling for complex scalar particles. The unparticle curves have the scalar unparticle coupling λ between unparticle and SM fields set to 1, with the scaling dimension $d_{\mathcal{U}}$ ranging from 1.5 to 2.1. The SM background $\mathrm{ZZ} \to \ell^{-}\ell^{+}\nu\overline{\nu}$ is shown as a red solid curve.

20 for the 2012 data sample.

4 Event reconstruction

Events are collected by requiring dilepton (ee or $\mu\mu$) triggers with thresholds of $p_{\mathrm{T}} > 17$ and 8 GeV for the leading and subleading leptons, respectively. Single-lepton triggers with thresholds of $p_{\mathrm{T}} > 27\,(24)$ GeV for electrons (muons) are also included to recover residual trigger inefficiencies. Prior to the selection of leptons, a primary vertex must be selected as the event vertex. The vertex with largest value of $\sum p_{\mathrm{T}}^2$ for the associated tracks is selected. Simulation studies show that this requirement correctly selects the event vertex in more than 99% of both signal and background events. The lepton candidate tracks are required to be compatible with the event vertex.

A particle-flow (PF) event algorithm [59, 60] reconstructs and identifies each individual particle with an optimized combination of information from the various elements of the CMS detector. The energy of photons is directly obtained from the ECAL measurement, corrected for zero-suppression effects. The energy of electrons is determined from a combination of the electron momentum at the event vertex as determined by the tracker, the energy of the corresponding ECAL cluster, and the energy sum of all bremsstrahlung photons spatially compatible with originating from the electron track. The energy of muons is obtained from the curvature of the corresponding track. The energy of charged hadrons is determined from a combination of its momentum measured in the tracker and the matching ECAL and HCAL energy deposits, corrected for zero-suppression effects and for the response function of the calorimeters to hadronic showers. Finally, the energy of neutral hadrons is obtained from the corresponding corrected ECAL and HCAL energy.

Electron candidates are reconstructed using two algorithms [40]: in the first, energy clusters

in the ECAL are matched to signals in the silicon tracker, and in the second, tracks in the silicon tracker are matched to ECAL clusters. The electron candidates used in the analysis are required to be reconstructed by both algorithms. To reduce the electron misidentification rate, the candidates have to satisfy additional identification criteria that are based on the shape of the electromagnetic shower in the ECAL. In addition, the electron track is required to originate from the event vertex and to match the shower cluster in the ECAL. Electron candidates with an ECAL cluster in the transition region between the ECAL barrel and end cap ($1.44 < |\eta| < 1.57$) are rejected because the reconstruction of an electron object in this region is not optimal. Candidates that are identified as coming from photon conversions [40] in the detector material are explicitly removed.

Muon candidate reconstruction is also based on two algorithms: in the first, tracks in the silicon tracker are matched with at least one muon segment in any detector plane of the muon system, and in the second algorithm, a combined fit is performed to hits in both the silicon tracker and the muon system [41]. The muon candidates in this analysis are required to be reconstructed by both algorithms and to be further identified as muons by the PF algorithm. To reduce the muon misidentification rate, additional identification criteria are applied based on the number of space points measured in the tracker and in the muon system, the fit quality of the muon track, and its consistency with the event vertex location.

Leptons produced in the decay of Z bosons are expected to be isolated from hadronic activity in the event. Therefore, an isolation requirement is applied based on the sum of the momenta of the PF candidates found in a cone of radius $R = \sqrt{(\Delta\eta)^2 + (\Delta\phi)^2} = 0.4$ around each lepton, where ϕ is the azimuthal angle. The isolation sum is required to be smaller than 15% (20%) of the p_{T} of the electron (muon). To correct for the contribution to the isolation sum from pileup interactions and the underlying event, a median energy density (ρ) is determined on an event-by-event basis using the method described in Ref. [61]. For each electron, the mean energy deposit in the isolation cone of the electron, coming from other pp collisions in the same bunch crossing, is estimated following the method described in Ref. [40], and subtracted from the isolation sum. For muon candidates, only charged tracks associated with the event vertex are included. The sum of the p_{T} for charged particles not associated with the event vertex in the cone of interest is rescaled by a factor corresponding to the average neutral to charge energy densities in jets and subtracted from the isolation sum.

Jets are reconstructed from PF candidates by using the anti-k_{T} clustering algorithm [62] with a distance parameter of 0.5, as implemented in the FASTJET package [63, 64]. Jets are found over the full calorimeter acceptance, $|\eta| < 5$. The jet momentum is defined as the vector sum of all particle momenta assigned to the jet and is found in the simulation to be within 5% to 10% of the true hadron-level momentum over the whole p_{T} range and detector acceptance. An overall energy subtraction is applied to correct for the extra energy clustered in jets due to pileup, following the procedure described in Ref. [65]. In the subtraction, the charged particle candidates associated with secondary vertices reconstructed in the event are also included. Other jet energy scale corrections applied are derived from simulation, and are confirmed by measurements of the energy balance in dijet and γ+jets events.

5 Event selection

An initial preselection with a large yield is used to validate the background model and is followed by a final selection that is designed to give maximal sensitivity to the signal. Selected events are required to have exactly two well-identified, isolated leptons with the same flavor

and opposite charge (e^+e^- or $\mu^+\mu^-$), each with $p_T > 20\,GeV$. The invariant mass of the lepton pair is required to be within $\pm 10\,GeV$ of the nominal mass of the Z boson. Only leptons within the pseudorapidity range of $|\eta| < 2.4\,(2.5)$ for muons (electrons) are considered. To reduce the background from the WZ process where the W boson decays leptonically, events are removed if an additional electron or muon is reconstructed with $p_T > 10\,GeV$. As a very loose preselection requirement, the dilepton transverse momentum ($p_T^{\ell\ell}$) is required to be larger than 50 GeV to reject the bulk of DY background events.

Since only a small amount of hadronic activity is expected in the final state of both DM and unparticle events, any event having two or more jets with $p_T > 30\,GeV$ is rejected. Top quark decays, which always involve the emission of b quarks, are further suppressed with the use of techniques based on soft-muon and b-jet tagging. The rejection of events with soft muons having $p_T > 3\,GeV$ reduces the background from semileptonic b decays. The b-jet tagging technique employed is based on the "combined secondary vertex" algorithm [66, 67]. This algorithm selects a group of tracks forming a secondary vertex within a jet and generates a likelihood discriminant to distinguish between b jets and jets originating from light quarks, gluons, or charm quarks. The applied threshold provides, on average, 80% efficiency for tagging jets originating from b quarks and 10% probability of light-flavor jet misidentification. The b-tagged jet is required to have $p_T > 20\,GeV$ and to be reconstructed within the tracker acceptance volume ($|\eta| < 2.5$).

The final selection is optimized for DM and unparticle signals to obtain the best expected cross section limit at 95% CL using four variables, E_T^{miss}, $\Delta\phi_{\ell\ell,\vec{p}_T^{\,miss}}$, $|E_T^{miss} - p_T^{\ell\ell}|/p_T^{\ell\ell}$, and $u_\parallel/p_T^{\ell\ell}$, where $u_\parallel$ is defined as the component of $\vec{u} = -\vec{p}_T^{\,miss} - \vec{p}_T^{\,\ell\ell}$ parallel to the direction of $\vec{p}_T^{\,\ell\ell}$. The last three variables effectively suppress background processes such as DY and top-quark production. If the best expected significance is used in the optimization, instead of the best expected limit, very similar results are obtained. In both electron and muon channels, a mass-independent event selection followed by a fit to the shape of the transverse mass $m_T = \sqrt{2p_T^{\ell\ell}E_T^{miss}(1-\cos\Delta\phi_{\ell\ell}}$ distribution is used to discriminate between the signal and the backgrounds. For each set of selection requirements considered, the full analysis, including the estimation of backgrounds and the systematic uncertainties, is repeated. The final selection criteria obtained after optimization for both the electron and muon channels are $E_T^{miss} > 80\,GeV$, $\Delta\phi_{\ell\ell,\vec{p}_T^{\,miss}} > 2.7$, $|u_\parallel/p_T^{\ell\ell}| < 1$, and $|E_T^{miss} - p_T^{\ell\ell}|/p_T^{\ell\ell} < 0.2$. This common selection is applied to both the DM and unparticle searches because the optimization results are very similar for both signals. A summary of the preselection and final selection criteria for the final analysis is listed in Table 1. Figure 4 shows the distributions of E_T^{miss} after preselection, in the ee and $\mu\mu$ channels. Good agreement is found between the observed distributions and the background prediction, which is described in the following section.

6 Background estimation

The ZZ and WZ backgrounds are modeled using MC simulation, and normalized to their respective NLO cross sections computed with MCFM 6.8 [68]. Other backgrounds, including $t\bar{t}$, tW, WW, $Z \to \tau\tau$, and DY are estimated from data for the final selection. The background from W+jets is negligible in the muon channel but significant in the electron channel, where an estimation method based on control samples in data is used for its estimation.

The background processes that do not involve Z boson production are referred to as nonresonant backgrounds. Such backgrounds arise mainly from leptonic W boson decays in $t\bar{t}$, tW, and WW events. There are also small contributions from *s*- and *t*-channel single top quark

Table 1: Summary of selections used in the analysis.

	Variable	Requirements
Preselection	p_{T}^{ℓ}	$>20\,\mathrm{GeV}$
	$\lvert m_{\ell\ell} - m_{\mathrm{Z}} \rvert$	$<10\,\mathrm{GeV}$
	Jet counting	≤ 1 jets with $p_{\mathrm{T}}^{\mathrm{j}} > 30\,\mathrm{GeV}$
	$p_{\mathrm{T}}^{\ell\ell}$	$>50\,\mathrm{GeV}$
	3rd-lepton veto	$p_{\mathrm{T}}^{\ell} > 10\,\mathrm{GeV}$
	Top quark veto	veto on b jets and soft muon
Selection	$\lvert u_{\parallel} / p_{\mathrm{T}}^{\ell\ell} \rvert$	<1
	$E_{\mathrm{T}}^{\mathrm{miss}}$	$>80\,\mathrm{GeV}$
	$\Delta\phi_{\ell\ell,\vec{p}_{\mathrm{T}}^{\mathrm{miss}}}$	>2.7 rad
	$\lvert E_{\mathrm{T}}^{\mathrm{miss}} - p_{\mathrm{T}}^{\ell\ell} \rvert / p_{\mathrm{T}}^{\ell\ell}$	<0.2

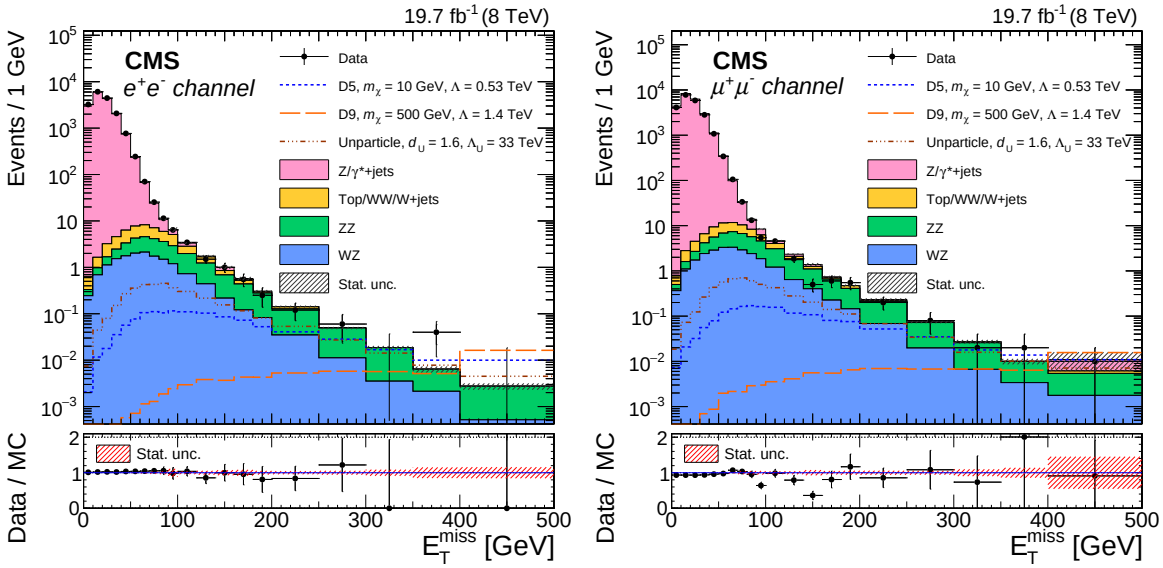

Figure 4: The distribution of $E_{\mathrm{T}}^{\mathrm{miss}}$ after preselection for the $\mathrm{Z} \to \mathrm{e}^{+}\mathrm{e}^{-}$ (left) and $\mathrm{Z} \to \mu^{+}\mu^{-}$ (right) channels. Expected signal distributions are shown for Dirac fermions with vector or tensor couplings and for unparticles. The total statistical uncertainty in the overall background is shown as a hatched region. The horizontal bars on the data points indicate the bin width. Overflow events are included in the rightmost bins.

events and $\mathrm{Z} \to \tau\tau$ events in which τ leptons produce electrons or muons and $E_{\mathrm{T}}^{\mathrm{miss}}$. We estimate these nonresonant backgrounds using a data control sample, consisting of events with an opposite-charge different-flavor dilepton pair ($\mathrm{e}^{\pm}\mu^{\mp}$) that otherwise pass the full selection. As the decay rates for $\mathrm{Z} \to \mathrm{e}^{+}\mathrm{e}^{-}$ and $\mathrm{Z} \to \mu^{+}\mu^{-}$ are equal, by equating the ratio of observed dilepton counts to the square of the ratio of efficiencies, the backgrounds in the ee and $\mu\mu$ channels can be estimated,

$$N_{\mathrm{bkg,ee}}^{\mathrm{est}} = N_{\mathrm{e}\mu}^{\mathrm{data,\,corr}}\, k_{\mathrm{ee}}, \qquad k_{\mathrm{ee}} = \frac{1}{2}\sqrt{\frac{N_{\mathrm{ee}}^{\mathrm{data}}}{N_{\mu\mu}^{\mathrm{data}}}},$$

$$N_{\mathrm{bkg},\mu\mu}^{\mathrm{est}} = N_{\mathrm{e}\mu}^{\mathrm{data,\,corr}}\, k_{\mu\mu}, \qquad k_{\mu\mu} = \frac{1}{2}\sqrt{\frac{N_{\mu\mu}^{\mathrm{data}}}{N_{\mathrm{ee}}^{\mathrm{data}}}},$$

in which the coefficient of $1/2$ in the correction factors k_{ee} and $k_{\mu\mu}$ comes from the dilepton

decay ratios for ee, $\mu\mu$, and eμ in these nonresonant backgrounds and N_{ee}^{data} and $N_{\mu\mu}^{data}$ are the numbers of selected ee and $\mu\mu$ events from data with masses inside the Z mass window. The ratio $\sqrt{N_{ee}^{data}/N_{\mu\mu}^{data}}$ and the reciprocal quantity take into account the difference between the electron and muon selection efficiencies. The term $N_{e\mu}^{data,\,corr}$ is the number of eμ events observed in data corrected by subtracting ZZ, WZ, DY, and W+jets background contributions estimated using MC simulation. The kinematic distributions of the estimated nonresonant backgrounds are taken from the distributions of the eμ sample with the overall normalization determined by the method described above. The validity of this procedure for predicting nonresonant backgrounds is checked with simulated events containing $t\bar{t}$, tW, WW, and $Z \to \tau\tau$ processes. We assign a systematic uncertainty of 17% (15%) to this background estimation in the electron (muon) channel, based on closure tests that compare the predictions obtained from the control sample with those from the simulated events.

The DY process is dominant in the region of low E_T^{miss}. This process does not produce undetectable particles, and therefore the measured E_T^{miss} arises from limited detector acceptance and mismeasurement. The estimation of this background uses simulated DY events, which are normalized to the data with scale factors obtained by measuring the number of DY events in background-dominated control regions, after subtracting other processes. These scale factors are of order 1.1–1.2. The control regions are defined with the full selection except for the requirements on E_T^{miss}, $\Delta\phi_{\ell\ell,\vec{p}_T^{\,miss}}$, and $|E_T^{miss} - p_T^{\ell\ell}|/p_T^{\ell\ell}$. The results are calculated independently for control regions with variables E_T^{miss} and $|E_T^{miss} - p_T^{\ell\ell}|/p_T^{\ell\ell}$ and compared with each other as part of the estimate of systematic uncertainty. Based on the variations of the estimates with the choice of control regions, a systematic uncertainty of 10% (11%) is assigned to the DY background estimate in the electron (muon) channel.

A W+jets background event consists of a genuine prompt lepton from the W decay and a nonisolated lepton resulting from the leptonic decay of heavy quarks, misidentified hadrons, or electrons from photon conversions. The rate at which jets are misidentified as leptons may not be accurately described in the MC simulation, so the rate of jets passing lepton identification requirements is determined using a control data sample enriched in jets. The genuine lepton contamination from W/Z+jets events in the selected control sample is subtracted using simulation to avoid biasing the calculation of the misidentification rate. The final estimation is obtained by applying these weights to a sample selected with lepton identification requirements that are looser than for the signal sample. The main source of systematic uncertainty for this background estimation comes from the measurement of the misidentification rate, which depends on the accuracy of the subtraction of real leptons in the control sample. A systematic uncertainty of 15% is assigned, based on the dependence of the calculated misidentification rates on the selection criteria applied to the control sample.

7 Efficiencies and systematic uncertainties

The efficiencies for selecting, reconstructing, and identifying isolated leptons are determined from simulation and then corrected with scale factors determined from applying a "tag-and-probe" technique [69] to $Z \to \ell^+\ell^-$ events. The trigger efficiencies for the electron and muon channels are found to be above 90%, varying as a function of p_T and $|\eta|$ of the lepton. The identification efficiency for electrons (muons), when applying the criteria described in Sec. 4, is found to be 95% (94%). The corresponding data-to-MC scale factors are typically in the range 0.94–1.01 (0.98–1.02) for the electron (muon) channel, depending on the p_T and $|\eta|$ of the lepton candidate. For both channels, the overall uncertainty in selecting and reconstructing leptons in an event is about 3%.

The systematic uncertainties include normalization uncertainties that affect the overall size of contributions, and shape uncertainties that alter the shapes of the distributions used in extracting the signal limits. The systematic uncertainties are summarized in Table 2.

Table 2: Summary of systematic uncertainties. Each background uncertainty represents the variation of the relative yields of the particular background components. The signal uncertainties represent the relative variations in the signal acceptance, and ranges quoted cover both signals of DM and unparticles with different DM masses or scaling dimensions. For shape uncertainties, the numbers correspond to the overall effect of the shape variation on yield or acceptance. The symbol — indicates that the systematic uncertainty is not applicable.

Source	Background uncertainty (%)	Signal uncertainty (%)
PDF+α_S	5–6	8–20
Factorization and renormalization scale	7–8	5
Acceptance (ZZ)	14	—
Integrated luminosity	2.6	2.6
Lepton trigger, reconstruction & identification, isolation	3	3
DY normalization	10–11	—
$\mathrm{t\bar{t}}$, tW, WW normalization	15–17	—
W+jets normalization	15–23	—
MC statistics (signal, ZZ, WZ)	1–2	1–2
Control region statistics (DY)	25	—
Control region statistics ($\mathrm{t\bar{t}}$, tW, WW)	18	—
Control region statistics (W+jets)	36	—
Pileup	0.5–1	0.1–0.7
b-jet tagging efficiency	0.4–1.4	0.6–1
Lepton momentum scale	0.4–0.5	0.1–1
Jet energy scale and resolution	5–7	3–5
Unclustered $E_{\mathrm{T}}^{\mathrm{miss}}$ scale	1–2	1

The normalization uncertainties in the background estimates from data are described in Sec. 6. The overall approach for the estimation of the PDF and α_S uncertainties (referred to as PDF+α_S in the following) adopts the interim recommendations of the PDF4LHC group and is used both for signal and the background [70–74]. This is the most important uncertainty for the signals. As the mass of the DM particles increases, the PDF+α_S uncertainty reaches 20%, which can be explained by the diminishing phase space for DM production and the rise of the corresponding uncertainty in the cross section. The efficiencies for signal, ZZ, and WZ processes are estimated using simulation, and the uncertainties in the corresponding yields are derived from variations of the renormalization and factorization scales, α_S, and choice of PDFs, in which the factorization and renormalization scales are assessed by varying the original scales of the process by factors of 0.5 and 2. Typical values for the signal extraction efficiency are found to be around 40%. The uncertainty related to the renormalization and factorization scales is 5% for signal and 7%–8% for ZZ and WZ processes. The effect of variations in α_S and the choice of PDFs is 5%–6% for the ZZ and WZ backgrounds. The uncertainty assigned to the luminosity measurement is 2.6% [38].

The contributions to the shape uncertainties come from the lepton momentum scale, the jet energy scale and resolution, the unclustered $E_{\mathrm{T}}^{\mathrm{miss}}$ scale, the b tagging efficiency, and the pileup modeling. Each corresponding uncertainty is calculated by varying the respective variable of interest within its own uncertainties and propagating the variations to the variable m_{T} using

the final selection. In the case of the lepton momentum scale, the uncertainty is computed by varying the momentum of the leptons by their uncertainties. The uncertainty in the muon momentum scale is 1%. For electrons, uncertainties of 0.6% for the barrel and 1.5% for the end caps are applied. For the ZZ background, cross checks are made using the generators MADGRAPH, POWHEG [75], and SHERPA 2.1.1 [76]. A comparison of the acceptance from normalized yields obtained with these generators is made in the signal region. In each bin of m_{T}, the maximum difference in acceptance with respect to the MADGRAPH prediction is assigned as a separate additional systematic uncertainty. The limit setting procedure discussed in Sec. 8 incorporates this acceptance uncertainty from each of the separate bins. The weighted average of these uncertainties is 14%. This is the dominant uncertainty in the total background prediction for the signal region. For the WZ background, this difference in acceptance is not observed, and data and simulation agree in the selected three-lepton control region.

The uncertainties in the calibration of the jet energy scale and resolution directly affect the assignments of jets to jet categories, the $E_{\mathrm{T}}^{\mathrm{miss}}$ computation, and all the selections related to jets. The effect of the jet energy scale uncertainty is estimated by varying the energy scale by $\pm 1\sigma$. A similar strategy is used to evaluate the systematic uncertainty related to the jet energy resolution. The uncertainties in the final yields are found to be 3%–5% (5%–7%) for signal (background). The effect of the uncertainty in the energy scale of the unclustered component of the $E_{\mathrm{T}}^{\mathrm{miss}}$ measurement is estimated by subtracting the leptons and jets from the $E_{\mathrm{T}}^{\mathrm{miss}}$ summation and by varying the residual recoil by $\pm 10\%$. The clustered component is then added back in order to recalculate the value of $E_{\mathrm{T}}^{\mathrm{miss}}$. The resultant uncertainty in the final yields is found to be of order 1%–2%. Since the b tagging efficiencies measured in data are somewhat different from those predicted by the simulation, an event-by-event reweighting using data-to-MC scale factors is applied to simulated events. The uncertainty associated with this procedure is obtained by varying the event-by-event weight by $\pm 1\sigma$. The total uncertainty in the final yields is 0.6–1% (0.4–1.4%) for signal (background). All simulated events are reweighted to reproduce the pileup conditions observed in data. To compute the uncertainty related to pileup modeling, we shift the mean of the distribution in simulation by 5%. The variation of the final yields induced by this procedure is less than 1%. For the processes estimated from simulation, the sizes of the MC samples limit the precision of the modeling, and the corresponding statistical uncertainty is incorporated into the shape uncertainty. A similar treatment is applied to the backgrounds estimated from control samples in data based on the statistical uncertainties in the corresponding control samples.

8 Results

For both the electron and the muon channels, a shape-based analysis is employed. The expected numbers of background and signal events scaled by a signal strength modifier are combined in a binned likelihood for each bin of the m_{T} distribution. The signal strength modifier, defined as the signal cross section divided by the cross section suggested by theory, determines the strength of the signal process. The numbers of observed and expected events are shown in Table 3, including the expectation for a selected mass point for each type of signal. Figure 5 shows the m_{T} distributions after the final selection. The observed distributions agree with the SM background predictions and no excess of events is observed.

Upper limits on the contribution of events from new physics are computed by using the modified frequentist approach $\mathrm{CL_s}$ [77, 78] based on asymptotic formulas [79, 80].

Table 3: Signal predictions, background estimates, and observed number of events. The DM signal yields are given for masses $m_\chi = 10$, 200, and 500 GeV and cutoff scales $\Lambda = 0.37$, 0.53, 0.48, and 1.4 TeV. The yields from an unparticle signal are presented with a scaling dimension $d_\mathcal{U} = 1.6$ and a renormalization scale $\Lambda_\mathcal{U} = 33$ TeV. The corresponding statistical and systematic uncertainties are shown, in that order.

Process	e^+e^-	$\mu^+\mu^-$
C3, $m_\chi = 10$ GeV, $\Lambda = 0.37$ TeV	$10.7 \pm 0.2 \pm 1.1$	$12.8 \pm 0.3 \pm 1.1$
D5, $m_\chi = 10$ GeV, $\Lambda = 0.53$ TeV	$10.0 \pm 0.3 \pm 1.1$	$12.3 \pm 0.3 \pm 1.1$
D8, $m_\chi = 200$ GeV, $\Lambda = 0.48$ TeV	$9.0 \pm 0.2 \pm 1.1$	$11.1 \pm 0.2 \pm 0.9$
D9, $m_\chi = 500$ GeV, $\Lambda = 1.4$ TeV	$2.67 \pm 0.03 \pm 0.41$	$2.81 \pm 0.03 \pm 0.26$
Unparticle, $d_\mathcal{U} = 1.6$, $\Lambda_\mathcal{U} = 33$ TeV	$19.0 \pm 0.3 \pm 1.3$	$25.6 \pm 0.4 \pm 1.7$
$Z/\gamma^* \to \ell^+\ell^-$	$8.2 \pm 1.9 \pm 0.8$	$8.6 \pm 3.0 \pm 1.0$
$WZ \to 3\ell\nu$	$25.1 \pm 0.5 \pm 2.8$	$40.7 \pm 0.7 \pm 4.5$
$ZZ \to 2\ell 2\nu$	$59 \pm 1 \pm 10$	$79 \pm 1 \pm 14$
$t\bar{t}/tW/WW/Z \to \tau\tau$	$18.7 \pm 3.4 \pm 3.3$	$22.9 \pm 2.3 \pm 3.4$
W+jets	$1.8 \pm 0.6 \pm 0.3$	—
Total background	$113 \pm 4 \pm 13$	$151 \pm 4 \pm 18$
Data	111	133

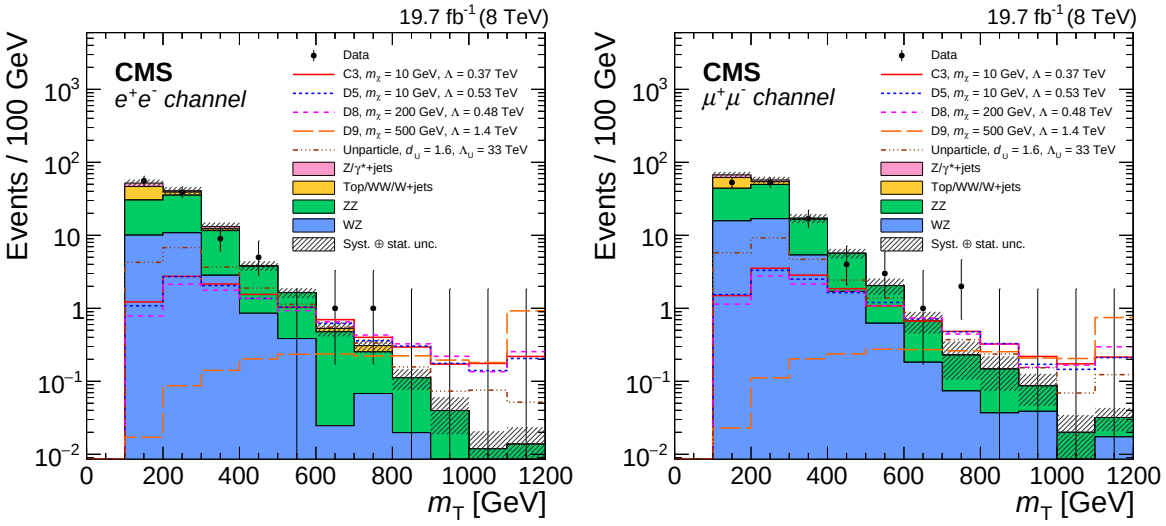

Figure 5: Distributions of the transverse mass for the final selection in the e^+e^- (left) and $\mu^+\mu^-$ (right) channels. Examples of expected signal distributions are shown for DM particle production and unparticle production. The total statistical and systematic uncertainty in the overall background is shown as a hatched region. Overflow events are included in the rightmost bins.

8.1 DM interpretation

The observed limit on the cross section for DM production depends on the DM particle mass and the nature of DM interactions with SM particles. Within the framework of effective field theory, the upper limits on this cross section can be translated into 90% CL lower limits on the effective cutoff scale Λ as a function of DM particle mass m_χ, as shown in Fig. 6. The choice of 90% CL is made in order to allow comparisons with direct detection experiments. The relic density of cold, nonbaryonic DM has been measured by Planck telescope [81] using the anisotropy of the cosmic microwave background and of the spatial distribution of galaxies. They obtain a value $\Omega h^2 = 0.1198 \pm 0.0026$, where h is the Hubble constant. The implications of this result plotted in the plane of the effective cutoff scale Λ and DM mass m_χ have been

calculated with MadDM 1.0 [82], and are shown in Fig. 6. Results from a search for DM particles using monojet signatures in CMS [14] are also plotted for comparison.

It has been emphasized by several authors [28, 83–85] that the effective field theory approach is not valid over the full range of phase space that is accessible at the LHC, since the scales involved can be comparable to the collision energy. In the LHC regime, the assumption of a pointlike interaction provides a reliable approximation of the underlying ultraviolet-complete theory only for appropriate choices of couplings and masses. To estimate the region of validity relevant to this analysis, we consider a simple tree-level ultraviolet-complete model that contains a massive mediator (M) exchanged in the s channel, with the couplings to quarks and DM particles described by coupling constants g_q and g_χ. The effective cutoff scale Λ thus can be expressed as $\Lambda \sim M/\sqrt{g_\mathrm{q} g_\chi}$, when momentum transfer is small ($Q_\mathrm{tr} < M$). Imposing a condition on the couplings $\sqrt{g_\mathrm{q} g_\chi} < 4\pi$ to ensure stability of the perturbative calculation and a mass requirement $M > 2m_\chi$, a lower bound $\Lambda > m_\chi/2\pi$ is obtained for the region of validity. The area below this boundary, where the effective theory of DM is not expected to provide a reliable prediction at the LHC, is shown as a pink shaded area in each of the panels of Fig. 6.

However, the requirement of $\Lambda > m_\chi/2\pi$ is not sufficient, according to some authors [83, 85–94], and the region of validity depends on the coupling values in the ultraviolet completion of the theory. Considering a more realistic minimum constraint $Q_\mathrm{tr} < M \sim \sqrt{g_\mathrm{q} g_\chi}\Lambda$, we can calculate the ratio R_Λ of the number of events fulfilling the validity criteria over all events produced in the accessible phase space,

$$R_\Lambda = \frac{\int_{p_\mathrm{T}^\mathrm{min}}^{p_\mathrm{T}^\mathrm{max}} \mathrm{d}p_\mathrm{T} \int_{\eta^\mathrm{min}}^{\eta^\mathrm{max}} \mathrm{d}\eta \left.\frac{\mathrm{d}^2\sigma_\mathrm{eff}}{\mathrm{d}p_\mathrm{T}\mathrm{d}\eta}\right|_{Q_\mathrm{tr} < \sqrt{g_\mathrm{q} g_\chi}\Lambda}}{\int_{p_\mathrm{T}^\mathrm{min}}^{p_\mathrm{T}^\mathrm{max}} \mathrm{d}p_\mathrm{T} \int_{\eta^\mathrm{min}}^{\eta^\mathrm{max}} \mathrm{d}\eta \frac{\mathrm{d}^2\sigma_\mathrm{eff}}{\mathrm{d}p_\mathrm{T}\mathrm{d}\eta}},$$

in which the values of R_Λ can be used to check the accuracy of the effective description in regions of parameter space (Λ, m_χ). Figure 6 includes the corresponding contours of $R_\Lambda = 80\%$ for all operators with couplings $\sqrt{g_\mathrm{q} g_\chi} = \pi$, and 4π. Alternatively, we can obtain the truncated limits by manually removing the events with $Q_\mathrm{tr} > \sqrt{g_\mathrm{q} g_\chi}\Lambda$ at the generator level. Figure 6 also shows these truncated limits with $\sqrt{g_\mathrm{q} g_\chi} = 1$. For a certain value of m_χ, the truncated limit goes to zero quickly because none of the events above this value fulfills the requirement $Q_\mathrm{tr} < \sqrt{g_\mathrm{q} g_\chi}\Lambda$. For a maximum coupling $g_{\chi,\mathrm{q}} = 4\pi$, 100% of the events passes this requirement, and the truncated limits coincide with the observed one and are not shown.

Figure 7 shows the 90% CL upper limits on the DM-nucleon cross section as a function of DM particle mass for both the spin-dependent and spin-independent cases [83, 95] obtained using the relations:

$$\sigma_0^\mathrm{D8,D9} = \sum_\mathrm{q} \frac{3\mu_{\chi N}^2}{\pi\Lambda^4} \left(\Delta_\mathrm{q}^N\right)^2 = 9.18 \times 10^{-40}\mathrm{cm}^2 \left(\frac{\mu_{\chi N}}{1\,\mathrm{GeV}}\right)^2 \left(\frac{300\,\mathrm{GeV}}{\Lambda}\right)^4,$$

$$\sigma_0^\mathrm{D5} = \sum_\mathrm{q} \frac{\mu_{\chi N}^2}{\pi\Lambda^4} \left(f_\mathrm{q}^N\right)^2 = 1.38 \times 10^{-37}\mathrm{cm}^2 \left(\frac{\mu_{\chi N}}{1\,\mathrm{GeV}}\right)^2 \left(\frac{300\,\mathrm{GeV}}{\Lambda}\right)^4,$$

$$\sigma_0^\mathrm{C3} = \sum_\mathrm{q} \frac{4\mu_{\chi N}^2}{\pi\Lambda^4} \left(f_\mathrm{q}^N\right)^2 = 5.52 \times 10^{-37}\mathrm{cm}^2 \left(\frac{\mu_{\chi N}}{1\,\mathrm{GeV}}\right)^2 \left(\frac{300\,\mathrm{GeV}}{\Lambda}\right)^4,$$

where $\mu_{\chi N}$ is the reduced mass of the DM-nucleon system, f_q^N characterizes the nucleon structure ($f_\mathrm{u}^p = f_\mathrm{d}^n = 2$ and $f_\mathrm{d}^p = f_\mathrm{u}^n = 1; f = 0$ otherwise), and Δ_q^N represents a spin-dependent form factor ($\Delta_\mathrm{u}^p = \Delta_\mathrm{d}^n = 0.842 \pm 0.012$, $\Delta_\mathrm{d}^p = \Delta_\mathrm{u}^n = -0.427 \pm 0.013$, $\Delta_\mathrm{s}^p = \Delta_\mathrm{s}^n = -0.085 \pm 0.018$)

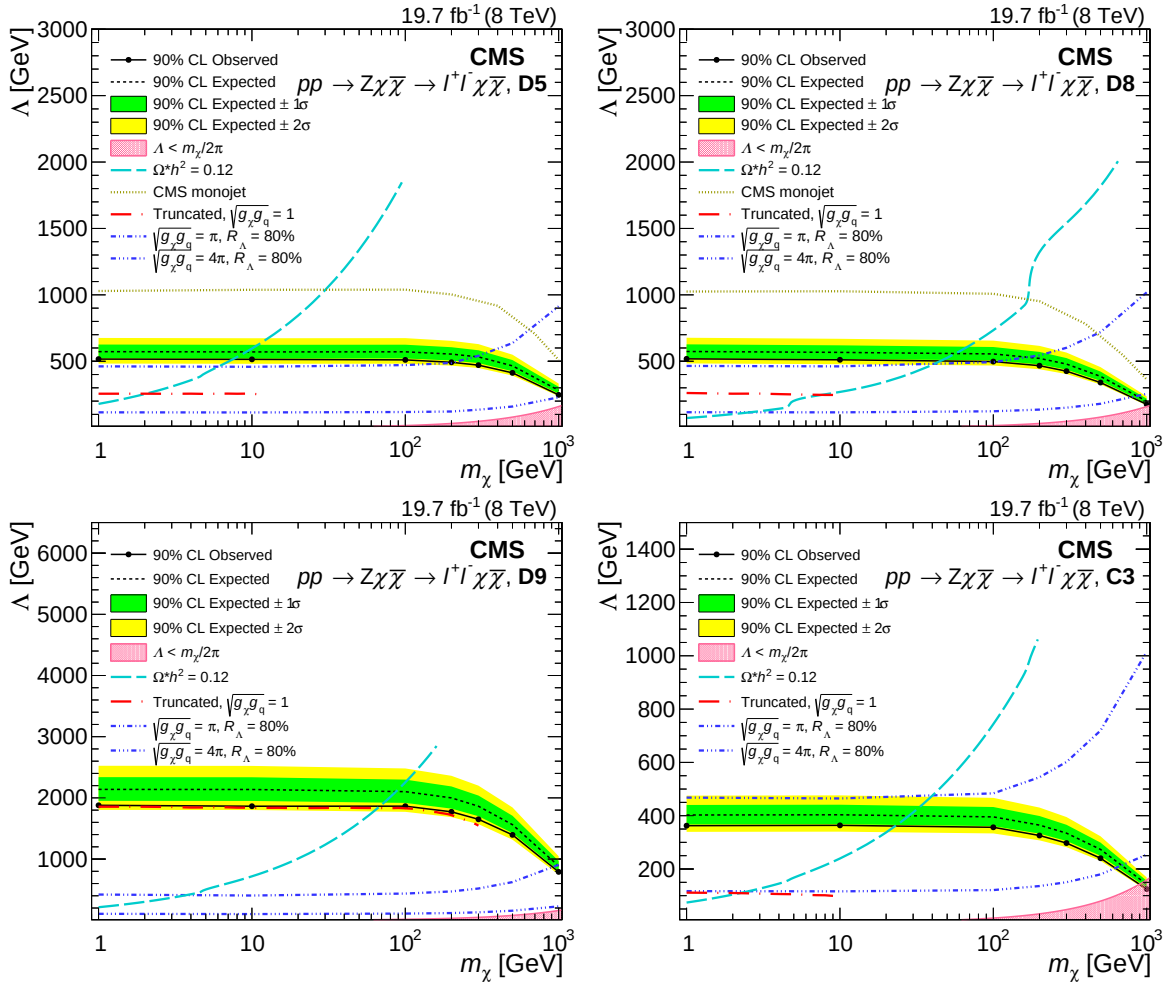

Figure 6: Expected and observed 90% CL lower limits on Λ as a function of DM particle mass m_χ for the operators D5 (top left), D8 (top right), D9 (bottom left), and C3 (bottom left). The pink shaded area is shown in each plot to indicate the lower bound $\Lambda > m_\chi/2\pi$ on the validity of the effective field theory DM model. The cyan long-dashed line calculated by MadDM 1.0 [82] reflects the relic density of cold, nonbaryonic DM: $\Omega h^2 = 0.1198 \pm 0.0026$ measured by the Planck telescope [81]. Monojet results from CMS [14] are shown for comparison. Truncated limits with $\sqrt{g_q g_\chi} = 1$ are presented with red dot long-dashed lines. The blue double-dot and triple-dot dashed lines indicate the contours of $R_\Lambda = 80\%$ for all operators with couplings $\sqrt{g_q g_\chi} = \pi$ and 4π.

as specified in Ref. [95]. The truncated limits for D5, D8, D9, and C3 with $\sqrt{g_q g_\chi} = 1$ are presented with dashed lines in the same shade as the untruncated ones. For comparison, direct search results as well as collider results from the CMS monojet [14] and monophoton [16] studies are shown. The recent limits from ATLAS [26] coincide very closely with the untruncated CMS limits on D9 and D5 operators. The ATLAS curves are not shown on the figure, since they would be difficult to distinguish by eye. Results are also shown from a search for the invisible decays of the Higgs boson [96], interpreted in a Higgs-portal model [97, 98], where a Higgs boson with a mass of 125 GeV acts as a mediator between scalar DM and SM particles. The central (solid) line corresponds to the Higgs-nucleon coupling value (0.326) from a lattice calculation [99], and the upper (dot-dashed) and lower (dashed) lines are maximum (0.629) and minimum (0.260) values from the MILC Collaboration [100].

The expected and observed limits on the effective cutoff scale Λ as a function of the DM particle mass m_χ are listed in Tables 4 and 5 for the operators D5 and D8. The values for the operators D9 and C3 are listed in Tables 6 and 7. The results are also shown in terms of limits on DM-nucleon cross sections $\sigma_{\chi N}$, to allow comparison with the results from direct searches for DM particles.

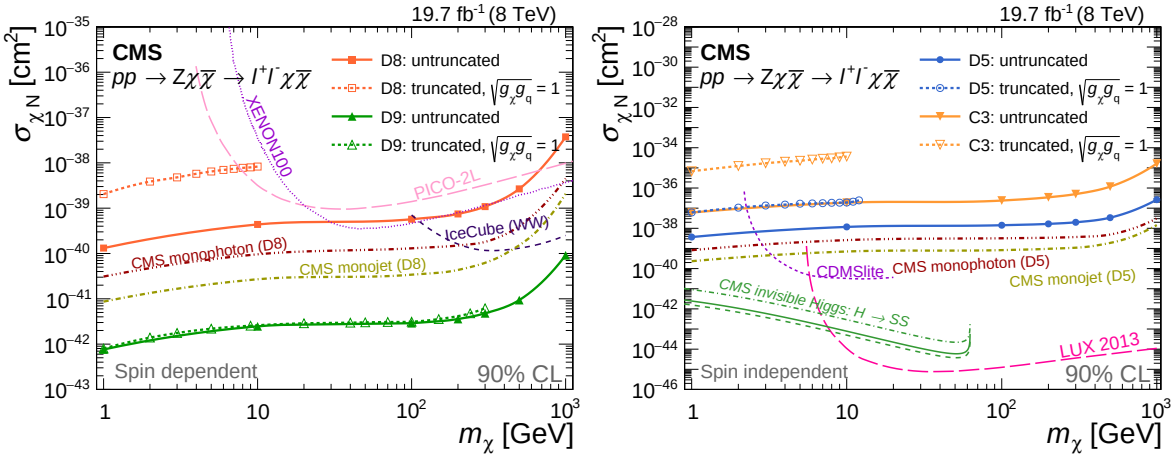

Figure 7: The 90% CL upper limits on the DM-nucleon cross section as a function of the DM particle mass. Left: spin-dependent limits for axial-vector (D8) and tensor (D9) coupling of Dirac fermion DM candidates, together with direct search experimental results from the PICO [101], XENON100 [102], and IceCube [7] collaborations. Right: spin-independent limits for vector coupling of complex scalar (C3) and Dirac fermion (D5) DM candidates, together with CDMSlite [8], LUX [11], as well as Higgs-portal scalar DM results from CMS [96] with central (solid), minimum (dashed) and maximum (dot dashed) values of Higgs-nucleon couplings. Collider results from CMS monojet [14] and monophoton [16] searches, interpreted in both spin-dependent and spin-independent scenarios, are shown for comparison. The truncated limits for D5, D8, D9, and C3 with $\sqrt{g_q g_\chi} = 1$ are presented with dashed lines in same shade as the untruncated ones.

Table 4: Expected and observed 90% CL upper limits on the DM-nucleon cross section $\sigma_{\chi N}$ and effective cutoff scale Λ for operator D5.

m_χ	Expected		Expected-1σ		Expected$+1\sigma$		Observed	
	Λ	$\sigma_{\chi N}$	Λ	$\sigma_{\chi N}$	Λ	$\sigma_{\chi N}$	Λ	$\sigma_{\chi N}$
(GeV)	(GeV)	(cm^2)	(GeV)	(cm^2)	(GeV)	(cm^2)	(GeV)	(cm^2)
1	572	2.4×10^{-39}	626	1.7×10^{-39}	522	3.5×10^{-39}	516	3.7×10^{-39}
10	570	7.8×10^{-39}	624	5.4×10^{-39}	520	1.1×10^{-38}	514	1.2×10^{-38}
100	571	9.1×10^{-39}	625	6.3×10^{-39}	521	1.3×10^{-38}	510	1.4×10^{-38}
200	554	1.0×10^{-38}	606	7.2×10^{-39}	505	1.5×10^{-38}	492	1.7×10^{-38}
300	533	1.2×10^{-38}	583	8.5×10^{-39}	486	1.7×10^{-38}	471	2.0×10^{-38}
500	465	2.1×10^{-38}	509	1.5×10^{-38}	425	3.0×10^{-38}	413	3.4×10^{-38}
1000	281	1.6×10^{-37}	308	1.1×10^{-37}	257	2.3×10^{-37}	247	2.6×10^{-37}

Figure 8 shows the limits from operators D5 and D8 translated into upper limits on the DM annihilation rate $\langle\sigma v\rangle$ relevant to indirect astrophysical searches [86], in which σ is the annihilation cross section, v is the relative velocity of the annihilating particles, and the quantity $\langle\sigma v\rangle$ is averaged over the distribution of the DM velocity. In this paper, a particular astrophysical environment with $\langle v^2\rangle = 0.24$ is considered, which corresponds to the epoch of the early universe when DM froze out, producing the thermal relic abundance. A 100% branching fraction

Table 5: Expected and observed 90% CL upper limits on the DM-nucleon cross section $\sigma_{\chi N}$ and effective cutoff scale Λ for operator D8.

m_χ	Expected		Expected-1σ		Expected$+1\sigma$		Observed	
(GeV)	Λ (GeV)	$\sigma_{\chi N}$ (cm^2)	Λ (GeV)	$\sigma_{\chi N}$ (cm^2)	Λ (GeV)	$\sigma_{\chi N}$ (cm^2)	Λ (GeV)	$\sigma_{\chi N}$ (cm^2)
1	574	8.8×10^{-41}	627	6.1×10^{-41}	523	1.3×10^{-40}	518	1.3×10^{-40}
10	567	2.9×10^{-40}	620	2.0×10^{-40}	517	4.2×10^{-40}	511	4.4×10^{-40}
100	555	3.7×10^{-40}	607	2.6×10^{-40}	507	5.3×10^{-40}	498	5.7×10^{-40}
200	522	4.8×10^{-40}	570	3.3×10^{-40}	476	6.9×10^{-40}	467	7.5×10^{-40}
300	479	6.7×10^{-40}	524	4.7×10^{-40}	437	9.7×10^{-40}	425	1.1×10^{-39}
500	386	1.6×10^{-39}	422	1.1×10^{-39}	352	2.3×10^{-39}	340	2.7×10^{-39}
1000	199	2.3×10^{-38}	218	1.6×10^{-38}	182	3.3×10^{-38}	176	3.7×10^{-38}

Table 6: Expected and observed 90% CL upper limits on the DM-nucleon cross section $\sigma_{\chi N}$ and effective cutoff scale Λ for operator D9.

m_χ	Expected		Expected-1σ		Expected$+1\sigma$		Observed	
(GeV)	Λ (GeV)	$\sigma_{\chi N}$ (cm^2)	Λ (GeV)	$\sigma_{\chi N}$ (cm^2)	Λ (GeV)	$\sigma_{\chi N}$ (cm^2)	Λ (GeV)	$\sigma_{\chi N}$ (cm^2)
1	2139	4.5×10^{-43}	2339	3.2×10^{-43}	1951	6.5×10^{-43}	1879	7.6×10^{-43}
10	2137	1.4×10^{-42}	2337	1.0×10^{-42}	1950	2.1×10^{-42}	1864	2.5×10^{-42}
100	2102	1.8×10^{-42}	2299	1.3×10^{-42}	1918	2.6×10^{-42}	1865	2.9×10^{-42}
200	2000	2.2×10^{-42}	2187	1.5×10^{-42}	1825	3.2×10^{-42}	1772	3.6×10^{-42}
300	1863	2.9×10^{-42}	2038	2.1×10^{-42}	1700	4.2×10^{-42}	1650	4.8×10^{-42}
500	1562	6.0×10^{-42}	1708	4.2×10^{-42}	1425	8.6×10^{-42}	1395	9.4×10^{-42}
1000	886	5.8×10^{-41}	969	4.0×10^{-41}	809	8.3×10^{-41}	790	9.1×10^{-41}

Table 7: Expected and observed 90% CL upper limits on the DM-nucleon cross section $\sigma_{\chi N}$ and effective cutoff scale Λ for operator C3.

m_χ	Expected		Expected-1σ		Expected$+1\sigma$		Observed	
(GeV)	Λ (GeV)	$\sigma_{\chi N}$ (cm^2)	Λ (GeV)	$\sigma_{\chi N}$ (cm^2)	Λ (GeV)	$\sigma_{\chi N}$ (cm^2)	Λ (GeV)	$\sigma_{\chi N}$ (cm^2)
1	403	4.0×10^{-38}	440	2.8×10^{-38}	367	5.7×10^{-38}	363	6.1×10^{-38}
10	403	1.2×10^{-37}	441	8.7×10^{-38}	368	1.8×10^{-37}	364	1.9×10^{-37}
100	396	1.6×10^{-37}	433	1.1×10^{-37}	361	2.3×10^{-37}	356	2.4×10^{-37}
200	365	2.2×10^{-37}	399	1.5×10^{-37}	333	3.2×10^{-37}	326	3.5×10^{-37}
300	335	3.1×10^{-37}	366	2.2×10^{-37}	305	4.5×10^{-37}	297	5.0×10^{-37}
500	273	7.0×10^{-37}	299	4.9×10^{-37}	250	1.0×10^{-36}	241	1.2×10^{-36}
1000	143	9.5×10^{-36}	156	6.6×10^{-36}	130	1.4×10^{-35}	125	1.6×10^{-35}

of DM annihilating to quarks is assumed. The corresponding truncated limits for D5 and D8 with coupling $\sqrt{g_q g_\chi} = 1$ are also presented with dashed lines in same shade as the untruncated ones. The value required for DM particles to make up the relic abundance is labeled "Thermal relic value" and is shown as a red dotted line. With this constraint on the annihilation rate, we can conclude that Dirac fermion DM is ruled out at 95% CL for $m_\chi < 6\,\text{GeV}$ in the case of vector coupling and $m_\chi < 30\,\text{GeV}$ in the case of axial-vector coupling. Indirect search results from H.E.S.S [103] and Fermi-LAT [104] are also shown for comparison. These results have been multiplied by a factor of 2 since they assume Majorana rather than Dirac fermions.

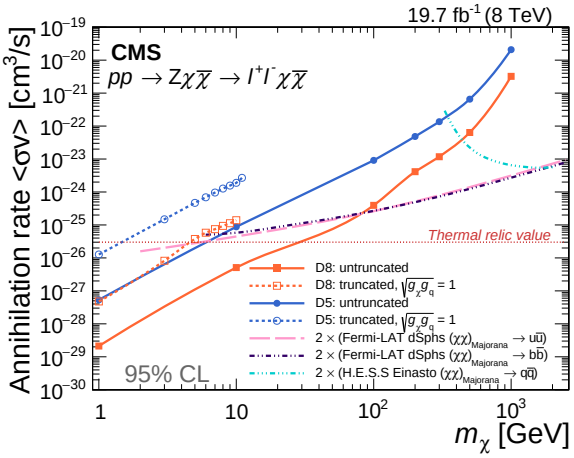

Figure 8: The 95% CL upper limits on the DM annihilation rate $\langle\sigma v\rangle$ for $\chi\overline{\chi} \to q\overline{q}$ as a function of the DM particle mass for vector (D5) and axial-vector (D8) couplings of Dirac fermion DM. A 100% branching fraction of DM annihilating to quarks is assumed. Indirect search experimental results from H.E.S.S [103] and Fermi-LAT [104] are also plotted. The value required for DM particles to account for the relic abundance is labeled "Thermal relic value" and is shown as a red dotted line. The truncated limits for D5 and D8 with $\sqrt{g_q g_\chi} = 1$ are presented with dashed lines in same shade as the untruncated ones.

8.2 Unparticle interpretation

In the scenario of the unparticle model, the 95% CL upper limits on the coupling constant λ between the unparticle and the SM fields with fixed effective cutoff scales $\Lambda_\mathcal{U} = 10$ TeV and 100 TeV, as functions of the scaling dimension $d_\mathcal{U}$, are shown on the left of Fig. 9. The right-hand plot of Fig. 9 presents 95% CL lower limits on the effective cutoff scale $\Lambda_\mathcal{U}$ with a fixed coupling $\lambda = 1$ and compares the result with the limits obtained from the CMS monojet search [14] and reinterpretation of LEP searches [37]. The search presented in this paper (labeled "monoZ") gives the most stringent limits. Tables 8 and 9 show the 95% CL upper limits on the coupling λ between unparticles and the SM fields for values of the scaling dimension $d_\mathcal{U}$ in the range from 1.01 to 2.2, and fixed effective cutoff scales of 10 TeV and 100 TeV. Lower limits at 95% CL on the effective cutoff scale $\Lambda_\mathcal{U}$ are given in Table 10, for $d_\mathcal{U}$ in the range from 1.6 to 2.2 and a fixed coupling $\lambda = 1$.

8.3 Model-independent limits

As an alternative to the interpretation of the results in specific models, a single-bin analysis is applied to obtain model-independent expected and observed 95% CL upper limits on the visible cross section $\sigma_{\text{vis}}^{\text{BSM}}$ for beyond the standard model (BSM) physics processes. The limits as a function of $E_{\text{T}}^{\text{miss}}$ thresholds are shown in Fig. 10. With a $E_{\text{T}}^{\text{miss}}$ threshold of 80 (150) GeV, we exclude the visible cross section $\sigma_{\text{vis}}^{\text{BSM}} > 2.5\,(0.85)$ fb. Table 11 shows the total SM background predictions for the numbers of events passing the selection requirements, for different $E_{\text{T}}^{\text{miss}}$ thresholds, compared with the observed numbers of events. The 95% CL expected and observed upper limits for the contribution of events from BSM sources are also shown.

9 Summary

A search for evidence for particle dark matter and unparticle production at the LHC has been performed in events containing two charged leptons, consistent with the decay of a Z boson,

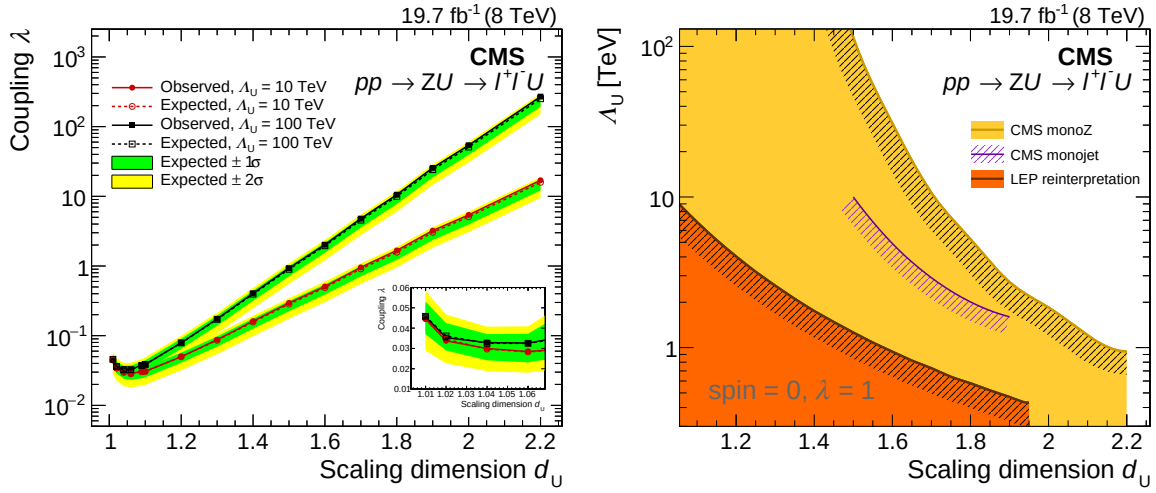

Figure 9: Left: 95% CL upper limits on the coupling λ between the unparticle and SM fields with fixed effective cutoff scales $\Lambda_{\mathcal{U}} = 10$ and 100 TeV. The plot inserted provides an expanded view of the limits at low scaling dimension. Right: 95% CL lower limits on unparticle effective cutoff scale $\Lambda_{\mathcal{U}}$ with a fixed coupling $\lambda = 1$. The results from CMS monojet [14] and reinterpretation of LEP searches [37] are also shown for comparison. The excluded region is indicated by the shading.

Table 8: Expected and observed 95% CL upper limits on the coupling λ between unparticles and the SM fields, for values of $d_{\mathcal{U}}$ in the range from 1.01 to 2.20 and a fixed effective cutoff scale $\Lambda_{\mathcal{U}} = 10$ TeV.

$d_{\mathcal{U}}$	λ			
	Expected	Expected-1σ	Expected$+1\sigma$	Observed
1.01	0.045	0.038	0.053	0.044
1.02	0.035	0.030	0.042	0.034
1.04	0.029	0.025	0.035	0.030
1.06	0.028	0.024	0.033	0.028
1.09	0.030	0.025	0.035	0.031
1.10	0.031	0.026	0.036	0.031
1.30	0.085	0.072	0.100	0.087
1.50	0.273	0.232	0.322	0.295
1.70	0.864	0.734	1.018	0.956
1.90	2.86	2.43	3.37	3.22
2.20	14.8	12.6	17.4	17.0

and large missing transverse momentum. The study is based on a data set corresponding to an integrated luminosity of 19.7 fb^{-1} of pp collisions collected by the CMS detector at a center-of-mass energy of 8 TeV. The results are consistent with the expected standard model contributions. These results are interpreted in two scenarios for physics beyond the standard model: dark matter and unparticles. Model-independent 95% confidence level upper limits are also set on contributions to the visible Z+$E_{\mathrm{T}}^{\mathrm{miss}}$ cross section from sources beyond the standard model. Upper limits at 90% confidence level are set on the DM-nucleon scattering cross sections as a function of DM particle mass for both spin-dependent and spin-independent cases. Limits are also set on the DM annihilation rate assuming a branching fraction of 100% for annihilation to quarks, and on the effective cutoff scale. In addition, the most stringent limits to date at 95% confidence level on the coupling between unparticles and the standard model fields as well as

Table 9: Expected and observed 95% CL upper limits on the coupling λ between unparticles and the SM fields, for values of $d_{\mathcal{U}}$ in the range from 1.01 to 2.20 and a fixed effective cutoff scale $\Lambda_{\mathcal{U}} = 100\,\text{TeV}$.

$d_{\mathcal{U}}$	λ			
	Expected	Expected-1σ	Expected$+1\sigma$	Observed
1.01	0.046	0.039	0.054	0.045
1.02	0.037	0.031	0.044	0.035
1.04	0.032	0.027	0.038	0.033
1.06	0.032	0.027	0.038	0.033
1.09	0.037	0.031	0.043	0.038
1.10	0.039	0.033	0.046	0.039
1.30	0.169	0.143	0.199	0.174
1.50	0.864	0.734	1.018	0.933
1.60	1.88	1.60	2.22	2.02
1.70	4.33	3.68	5.10	4.79
1.90	22.7	19.3	26.8	25.6
2.20	235	199	276	270

Table 10: Expected and observed 95% CL lower limits on the effective cutoff scale $\Lambda_{\mathcal{U}}$ for values of $d_{\mathcal{U}}$ in the range from 1.60 to 2.20 and a fixed coupling $\lambda = 1$.

$d_{\mathcal{U}}$	$\Lambda_{\mathcal{U}}$ (TeV)			
	Expected	Expected-1σ	Expected$+1\sigma$	Observed
1.50	134	186	96.4	115
1.60	34.8	45.7	26.5	30.9
1.70	12.3	15.6	9.75	10.7
1.80	6.08	7.45	4.95	5.25
1.90	3.11	3.72	2.59	2.72
2.00	2.09	2.46	1.77	1.85
2.20	1.06	1.21	0.92	0.94

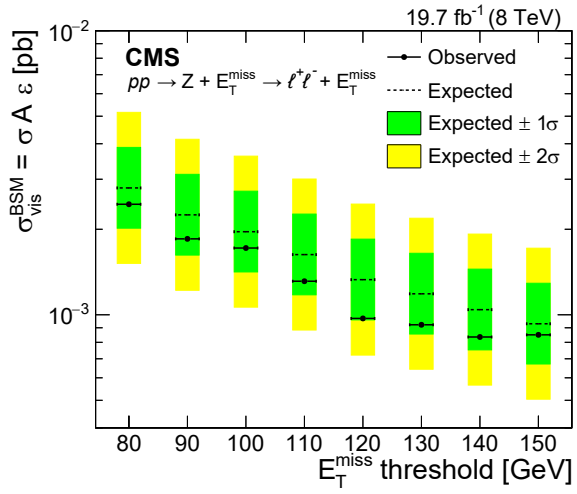

Figure 10: The model-independent upper limits at 95% CL on the visible cross section ($\sigma\, A\, \epsilon$) for BSM production of events, as a function of $E_{\mathrm{T}}^{\mathrm{miss}}$ threshold.

the effective cutoff scale as a function of the unparticle scaling dimension are obtained in this analysis.

Table 11: Total SM background predictions for the numbers of events passing the selection requirements, for different $E_{\mathrm{T}}^{\mathrm{miss}}$ thresholds, compared with the observed numbers of events. The listed uncertainties include both statistical and systematic components. The 95% CL observed and expected upper limits for the contribution of events from BSM sources are also shown. The $\pm 1\sigma$ and $\pm 2\sigma$ excursions from expected limits are also given.

$E_{\mathrm{T}}^{\mathrm{miss}}$ (GeV) threshold	80	90	100	110	120	130	140	150
Total SM	263	193	150	117	90.5	72.5	59.2	45.1
Total uncertainty	$\pm$30	$\pm$24	$\pm$20	$\pm$16	$\pm$13	$\pm$12	$\pm$9.6	$\pm$7.6
Data	244	172	141	104	74	61	50	43
Obs. upper limit	48.3	36.5	33.8	25.9	19.1	18.2	16.5	16.7
Exp. upper limit +2σ	102	81.7	71.3	59.2	48.3	43.1	37.9	33.8
Exp. upper limit +1σ	76.5	61.5	53.7	44.6	36.4	32.4	28.5	25.4
Exp. upper limit	55.1	44.3	38.6	32.1	26.2	23.4	20.5	18.3
Exp. upper limit -1σ	39.7	32.0	27.9	23.2	18.9	16.9	14.8	13.2
Exp. upper limit -2σ	29.9	24.0	21.0	17.4	14.2	12.7	11.1	9.90

Acknowledgments

We congratulate our colleagues in the CERN accelerator departments for the excellent performance of the LHC and thank the technical and administrative staffs at CERN and at other CMS institutes for their contributions to the success of the CMS effort. In addition, we gratefully acknowledge the computing centers and personnel of the Worldwide LHC Computing Grid for delivering so effectively the computing infrastructure essential to our analyses. Finally, we acknowledge the enduring support for the construction and operation of the LHC and the CMS detector provided by the following funding agencies: the Austrian Federal Ministry of Science, Research and Economy and the Austrian Science Fund; the Belgian Fonds de la Recherche Scientifique and Fonds voor Wetenschappelijk Onderzoek; the Brazilian Funding Agencies (CNPq, CAPES, FAPERJ, and FAPESP); the Bulgarian Ministry of Education and Science; CERN; the Chinese Academy of Sciences, Ministry of Science and Technology, and National Natural Science Foundation of China; the Colombian Funding Agency (COLCIENCIAS); the Croatian Ministry of Science, Education and Sport, and the Croatian Science Foundation; the Research Promotion Foundation, Cyprus; the Ministry of Education and Research, Estonian Research Council via IUT23-4 and IUT23-6 and European Regional Development Fund, Estonia; the Academy of Finland, Finnish Ministry of Education and Culture, and Helsinki Institute of Physics; the Institut National de Physique Nucléaire et de Physique des Particules/CNRS and Commissariat à l'Énergie Atomique et aux Énergies Alternatives/CEA, France; the Bundesministerium für Bildung und Forschung, Deutsche Forschungsgemeinschaft, and Helmholtz-Gemeinschaft Deutscher Forschungszentren, Germany; the General Secretariat for Research and Technology, Greece; the National Scientific Research Foundation, and National Innovation Office, Hungary; the Department of Atomic Energy and the Department of Science and Technology, India; the Institute for Studies in Theoretical Physics and Mathematics, Iran; the Science Foundation, Ireland; the Istituto Nazionale di Fisica Nucleare, Italy; the Ministry of Science, ICT and Future Planning, and National Research Foundation (NRF), Republic of Korea; the Lithuanian Academy of Sciences; the Ministry of Education, and University of Malaya, Malaysia; the Mexican Funding Agencies (CINVESTAV, CONACYT, SEP, and UASLP-FAI); the Ministry of Business, Innovation and Employment, New Zealand; the Pakistan Atomic Energy Commission; the Ministry of Science and Higher Education and the National Science Centre, Poland; the Fundação para a Ciência e a Tecnologia, Portugal; JINR, Dubna, the Ministry of Education and Science of the Russian Federation, the Federal Agency of

Atomic Energy of the Russian Federation, Russian Academy of Sciences, and the Russian Foundation for Basic Research; the Ministry of Education, Science and Technological Development of Serbia; the Secretaría de Estado de Investigación, Desarrollo e Innovación and Programa Consolider-Ingenio 2010, Spain; the Swiss Funding Agencies (ETH Board, ETH Zurich, PSI, SNF, UniZH, Canton Zurich, and SER); the Ministry of Science and Technology, Taipei; the Thailand Center of Excellence in Physics, the Institute for the Promotion of Teaching Science and Technology of Thailand, Special Task Force for Activating Research, and the National Science and Technology Development Agency of Thailand; the Scientific and Technical Research Council of Turkey and Turkish Atomic Energy Authority; the National Academy of Sciences of Ukraine and State Fund for Fundamental Researches, Ukraine; the Science and Technology Facilities Council, United Kingdom; the US Department of Energy and the US National Science Foundation.

Individuals have received support from the Marie-Curie program and the European Research Council and EPLANET (European Union); the Leventis Foundation; the A. P. Sloan Foundation; the Alexander von Humboldt Foundation; the Belgian Federal Science Policy Office; the Fonds pour la Formation à la Recherche dans l'Industrie et dans l'Agriculture (FRIA-Belgium); the Agentschap voor Innovatie door Wetenschap en Technologie (IWT-Belgium); the Ministry of Education, Youth and Sports (MEYS) of the Czech Republic; the Council of Science and Industrial Research, India; the HOMING PLUS program of the Foundation for Polish Science, cofinanced by the European Union, Regional Development Fund; the OPUS program of the National Science Center (Poland); the Compagnia di San Paolo (Torino); MIUR Project No. 20108T4XTM (Italy); the Thalis and Aristeia programs cofinanced by EU-ESF and the Greek NSRF; the National Priorities Research Program by Qatar National Research Fund; the Rachadapisek Sompot Fund for Postdoctoral Fellowship, Chulalongkorn University (Thailand); and the Welch Foundation, Contract No. C-1845.

References

[1] R. W. Tucker and C. Wang, "Dark matter gravitational interactions", *Class. Quant. Grav.* **15** (1998) 933, doi:10.1088/0264-9381/15/4/015, arXiv:gr-qc/9612019.

[2] M. Lopez-Corredoira, J. E. Beckman, and E. Casuso, "High-velocity clouds as dark matter in the local group", *Astron. Astrophys.* **351** (1999) 920, arXiv:astro-ph/9909389.

[3] D. Clowe et al., "A Direct Empirical Proof of The Existence of Dark Matter", *Astrophys. J.* **648** (2006) 109, doi:10.1086/508162, arXiv:astro-ph/0608407.

[4] PICASSO Collaboration, "Constraints on low-mass WIMP interactions on ^{19}F from PICASSO", *Phys. Lett. B* **711** (2012) 153, doi:10.1016/j.physletb.2012.03.078, arXiv:1202.1240.

[5] SIMPLE Collaboration, "Final Analysis and Results of the Phase II SIMPLE Dark Matter Search", *Phys. Rev. Lett.* **108** (2012) 201302, doi:10.1103/PhysRevLett.108.201302, arXiv:1106.3014.

[6] COUPP Collaboration, "First dark matter search results from a 4-kg CF_3I Bubble Chamber Operated in a Deep Underground site", *Phys. Rev. D* **86** (2012) 052001, doi:10.1103/PhysRevD.86.052001, arXiv:1204.3094.

[7] IceCube Collaboration, "Multi-year search for dark matter annihilations in the Sun with the AMANDA-II and IceCube detectors", *Phys. Rev. D* **85** (2012) 042002, doi:10.1103/PhysRevD.85.042002, arXiv:1112.1840.

[8] SuperCDMS Collaboration, "Search for Low-Mass Weakly Interacting Massive Particles Using Voltage-Assisted Calorimetric Ionization Detection in the SuperCDMS Experiment", *Phys. Rev. Lett.* **112** (2014) 041302, doi:10.1103/PhysRevLett.112.041302, arXiv:1309.3259.

[9] P. Cushman et al., "Snowmass CF1 Summary: WIMP Dark Matter Direct Detection", (2013). arXiv:1310.8327.

[10] SuperCDMS Collaboration, "Search for Low-Mass WIMPs with SuperCDMS", *Phys. Rev. Lett.* **112** (2014) 241302, doi:10.1103/PhysRevLett.112.241302, arXiv:1402.7137.

[11] LUX Collaboration, "First Results from the LUX Dark Matter Experiment at the Sanford Underground Research Facility", *Phys. Rev. Lett.* **112** (2014) 091303, doi:10.1103/PhysRevLett.112.091303, arXiv:1310.8214.

[12] Fermi-LAT Collaboration, "Constraining Dark Matter Models from a Combined Analysis of Milky Way Satellites with the Fermi Large Area Telescope", *Phys. Rev. Lett.* **107** (2011) 241302, doi:10.1103/PhysRevLett.107.241302, arXiv:1108.3546.

[13] J. Buckley et al., "Indirect Dark Matter Detection CF2 Working Group Summary", (2013). arXiv:1310.7040.

[14] CMS Collaboration, "Search for dark matter, extra dimensions, and unparticles in monojet events in proton-proton collisions at $\sqrt{s} = 8$ TeV", *Eur. Phys. J. C* **75** (2015) 235, doi:10.1140/epjc/s10052-015-3451-4, arXiv:1408.3583.

[15] ATLAS Collaboration, "Search for new phenomena in final states with an energetic jet and large missing transverse momentum in pp collisions at $\sqrt{s} = 8$ TeV with the ATLAS detector", *Eur. Phys. J. C* **75** (2015) 299, doi:10.1140/epjc/s10052-015-3517-3, arXiv:1502.01518.

[16] CMS Collaboration, "Search for new phenomena in monophoton final states in proton-proton collisions at $\sqrt{s} = 8$ TeV", *Phys. Lett. B* **755** (2016) 102, doi:10.1016/j.physletb.2016.01.057, arXiv:1410.8812.

[17] ATLAS Collaboration, "Search for new phenomena in events with a photon and missing transverse momentum in pp collisions at $\sqrt{s} = 8$ TeV with the ATLAS detector", *Phys. Rev. D* **91** (2015) 012008, doi:10.1103/PhysRevD.91.012008, arXiv:1411.1559.

[18] CMS Collaboration, "Search for physics beyond the standard model in final states with a lepton and missing transverse energy in proton-proton collisions at $\sqrt{s} = 8$ TeV", *Phys. Rev. D* **91** (2015) 092005, doi:10.1103/PhysRevD.91.092005, arXiv:1408.2745.

[19] ATLAS Collaboration, "Search for dark matter in events with heavy quarks and missing transverse momentum in pp collisions with the ATLAS detector", *Eur. Phys. J. C* **75** (2015) 92, doi:10.1140/epjc/s10052-015-3306-z, arXiv:1410.4031.

[20] ATLAS Collaboration, "Search for dark matter in events with a hadronically decaying W or Z boson and missing transverse momentum in pp collisions at $\sqrt{s}$ = 8 TeV with the ATLAS detector", *Phys. Rev. Lett.* **112** (2014) 041802, doi:10.1103/PhysRevLett.112.041802, arXiv:1309.4017.

[21] ATLAS Collaboration, "Search for new particles in events with one lepton and missing transverse momentum in pp collisions at $\sqrt{s}$ = 8 TeV with the ATLAS detector", *JHEP* **09** (2014) 037, doi:10.1007/JHEP09(2014)037, arXiv:1407.7494.

[22] ATLAS Collaboration, "Search for invisible particles produced in association with single-top-quarks in proton-proton collisions at $\sqrt{s}$ = 8 TeV with the ATLAS detector", *Eur. Phys. J. C* **75** (2015) 79, doi:10.1140/epjc/s10052-014-3233-4, arXiv:1410.5404.

[23] ATLAS Collaboration, "Search for Dark Matter in Events with Missing Transverse Momentum and a Higgs Boson Decaying to Two Photons in pp Collisions at $\sqrt{s} = 8$ TeV with the ATLAS Detector", *Phys. Rev. Lett.* **115** (2015) 131801, doi:10.1103/PhysRevLett.115.131801, arXiv:1506.01081.

[24] CMS Collaboration, "Search for Monotop Signatures in Proton-Proton Collisions at $\sqrt{s} = 8$ TeV", *Phys. Rev. Lett.* **114** (2015) 101801, doi:10.1103/PhysRevLett.114.101801, arXiv:1410.1149.

[25] CMS Collaboration, "Search for the production of dark matter in association with top-quark pairs in the single-lepton final state in proton-proton collisions at $\sqrt{s}$ = 8 TeV", *JHEP* **06** (2015) 121, doi:10.1007/JHEP06(2015)121, arXiv:1504.03198.

[26] ATLAS Collaboration, "Search for dark matter in events with a Z boson and missing transverse momentum in pp collisions at $\sqrt{s}$ = 8 TeV with the ATLAS detector", *Phys. Rev. D* **90** (2014) 012004, doi:10.1103/PhysRevD.90.012004, arXiv:1404.0051.

[27] L. M. Carpenter et al., "Collider searches for dark matter in events with a Z boson and missing energy", *Phys. Rev. D* **87** (2013) 074005, doi:10.1103/PhysRevD.87.074005, arXiv:1212.3352.

[28] J. Goodman et al., "Constraints on dark matter from colliders", *Phys. Rev. D* **82** (2010) 116010, doi:10.1103/PhysRevD.82.116010, arXiv:1008.1783.

[29] H. Georgi, "Unparticle physics", *Phys. Rev. Lett.* **98** (2007) 221601, doi:10.1103/PhysRevLett.98.221601, arXiv:hep-ph/0703260.

[30] H. Georgi, "Another odd thing about unparticle physics", *Phys. Lett. B* **650** (2007) 275, doi:10.1016/j.physletb.2007.05.037, arXiv:0704.2457.

[31] K. Cheung, W.-Y. Keung, and T.-C. Yuan, "Collider signals of unparticle physics", *Phys. Rev. Lett.* **99** (2007) 051803, doi:10.1103/PhysRevLett.99.051803, arXiv:0704.2588.

[32] K. Cheung, W.-Y. Keung, and T.-C. Yuan, "Collider Phenomenology of Unparticle Physics", *Phys. Rev. D* **76** (2007) 055003, doi:10.1103/PhysRevD.76.055003, arXiv:0706.3155.

[33] Z. Kang, "Upgrading sterile neutrino dark matter to FImP using scale invariance", *Eur. Phys. J. C* **75** (2015) 471, doi:10.1140/epjc/s10052-015-3702-4, arXiv:1411.2773.

[34] M. Rinaldi, G. Cognola, L. Vanzo, and S. Zerbini, "Inflation in scale-invariant theories of gravity", *Phys. Rev. D* **91** (2015) 123527, doi:10.1103/PhysRevD.91.123527, arXiv:1410.0631.

[35] H. Cheng, "The Possible Existence of Weyl's Vector Meson", *Phys. Rev. Lett.* **61** (1988) 2182, doi:10.1103/PhysRevLett.61.2182.

[36] T. Banks and A. Zaks, "On the phase structure of vector-like gauge theories with massless fermions", *Nucl. Phys. B* **196** (1982) 189, doi:10.1016/0550-3213(82)90035-9.

[37] S. Kathrein, S. Knapen, and M. J. Strassler, "Bounds from LEP on unparticle interactions with electroweak bosons", *Phys. Rev. D* **84** (2011) 015010, doi:10.1103/PhysRevD.84.015010, arXiv:1012.3737.

[38] CMS Collaboration, "CMS Luminosity Based on Pixel Cluster Counting - Summer 2013 Update", CMS Physics Analysis Summary CMS-PAS-LUM-13-001, 2013.

[39] CMS Collaboration, "The CMS experiment at the CERN LHC", *JINST* **3** (2008) S08004, doi:10.1088/1748-0221/3/08/S08004.

[40] CMS Collaboration, "Performance of electron reconstruction and selection with the CMS detector in proton-proton collisions at $\sqrt{s} = 8$ TeV", *JINST* **10** (2015) 06005, doi:10.1088/1748-0221/10/06/P06005, arXiv:1502.02701.

[41] CMS Collaboration, "Performance of CMS muon reconstruction in pp collision events at $\sqrt{s} = 7$ TeV", *JINST* **7** (2012) 10002, doi:10.1088/1748-0221/7/10/P10002, arXiv:1206.4071.

[42] J. Alwall et al., "The automated computation of tree-level and next-to-leading order differential cross sections, and their matching to parton shower simulations", *JHEP* **07** (2014) 079, doi:10.1007/JHEP07(2014)079, arXiv:1405.0301.

[43] T. Sjöstrand, S. Mrenna, and P. Skands, "PYTHIA 6.4 physics and manual", *JHEP* **05** (2006) 026, doi:10.1088/1126-6708/2006/05/026, arXiv:hep-ph/0603175.

[44] J. Pumplin et al., "New generation of parton distributions with uncertainties from global QCD analysis", *JHEP* **07** (2002) 012, doi:10.1088/1126-6708/2002/07/012, arXiv:hep-ph/0201195.

[45] R. Field, "Early LHC Underlying Event Data - Findings and Surprises", in *Hadron collider physics. Proceedings, 22nd Conference, HCP 2010, Toronto, Canada, August 23-27*. 2010. arXiv:1010.3558.

[46] T. Sjöstrand, S. Mrenna, and P. Z. Skands, "A brief introduction to PYTHIA 8.1", *Comput. Phys. Commun.* **178** (2008) 852, doi:10.1016/j.cpc.2008.01.036, arXiv:0710.3820.

[47] S. Ask, "Simulation of Z plus graviton/unparticle production at the LHC", *Eur. Phys. J. C* **60** (2009) 509, doi:10.1140/epjc/s10052-009-0949-7, arXiv:0809.4750.

[48] S. Ask et al., "Real emission and virtual exchange of gravitons and unparticles in PYTHIA8", *Comput. Phys. Commun.* **181** (2010) 1593, doi:10.1016/j.cpc.2010.05.013, arXiv:0912.4233.

[49] R. Corke and T. Sjöstrand, "Interleaved parton showers and tuning prospects", *JHEP* **03** (2011) 032, doi:10.1007/JHEP03(2011)032, arXiv:1011.1759.

[50] P. Nason, "A New method for combining NLO QCD with shower Monte Carlo algorithms", *JHEP* **11** (2004) 040, doi:10.1088/1126-6708/2004/11/040, arXiv:hep-ph/0409146.

[51] S. Frixione, P. Nason, and C. Oleari, "Matching NLO QCD computations with Parton Shower simulations: the POWHEG method", *JHEP* **11** (2007) 070, doi:10.1088/1126-6708/2007/11/070, arXiv:0709.2092.

[52] S. Alioli, P. Nason, C. Oleari, and E. Re, "A general framework for implementing NLO calculations in shower Monte Carlo programs: the POWHEG BOX", *JHEP* **06** (2010) 043, doi:10.1007/JHEP06(2010)043, arXiv:1002.2581.

[53] E. Re, "Single-top *Wt*-channel production matched with parton showers using the POWHEG method", *Eur. Phys. J. C* **71** (2011) 1547, doi:10.1140/epjc/s10052-011-1547-z, arXiv:1009.2450.

[54] S. Alioli, S.-O. Moch, and P. Uwer, "Hadronic top-quark pair-production with one jet and parton showering", *JHEP* **01** (2012) 137, doi:10.1007/JHEP01(2012)137, arXiv:1110.5251.

[55] J. Alwall et al., "MadGraph/MadEvent v4: the new web generation", *JHEP* **09** (2007) 028, doi:10.1088/1126-6708/2007/09/028, arXiv:0706.2334.

[56] H.-L. Lai et al., "Uncertainty induced by QCD coupling in the CTEQ global analysis of parton distributions", *Phys. Rev. D* **82** (2010) 054021, doi:10.1103/PhysRevD.82.054021, arXiv:1004.4624.

[57] H.-L. Lai et al., "New parton distributions for collider physics", *Phys. Rev. D* **82** (2010) 074024, doi:10.1103/PhysRevD.82.074024, arXiv:1007.2241.

[58] GEANT4 Collaboration, "GEANT4—a simulation toolkit", *Nucl. Instrum. Meth. A* **506** (2003) 250, doi:10.1016/S0168-9002(03)01368-8.

[59] CMS Collaboration, "Particle–Flow Event Reconstruction in CMS and Performance for Jets, Taus, and $E_{\mathrm{T}}^{\mathrm{miss}}$", CMS Physics Analysis Summary CMS-PAS-PFT-09-001, 2009.

[60] CMS Collaboration, "Commissioning of the Particle-flow Event Reconstruction with the first LHC collisions recorded in the CMS detector", CMS Physics Analysis Summary CMS-PAS-PFT-10-001, 2010.

[61] M. Cacciari and G. P. Salam, "Pileup subtraction using jet areas", *Phys. Lett. B* **659** (2008) 119, doi:10.1016/j.physletb.2007.09.077, arXiv:0707.1378.

[62] M. Cacciari, G. P. Salam, and G. Soyez, "The anti-k_t jet clustering algorithm", *JHEP* **04** (2008) 063, doi:10.1088/1126-6708/2008/04/063, arXiv:0802.1189.

[63] M. Cacciari, G. P. Salam, and G. Soyez, "FastJet user manual", *Eur. Phys. J. C* **72** (2012) 1896, doi:10.1140/epjc/s10052-012-1896-2, arXiv:1111.6097.

[64] M. Cacciari and G. P. Salam, "Dispelling the N^3 myth for the k_t jet-finder", *Phys. Lett. B* **641** (2006) 57, doi:10.1016/j.physletb.2006.08.037, arXiv:hep-ph/0512210.

[65] CMS Collaboration, "Determination of jet energy calibration and transverse momentum resolution in CMS", *JINST* **6** (2011) P11002, doi:10.1088/1748-0221/6/11/P11002, arXiv:1107.4277.

[66] CMS Collaboration, "Identification of b-quark jets with the CMS experiment", *JINST* **8** (2013) 04013, doi:10.1088/1748-0221/8/04/P04013, arXiv:1211.4462.

[67] CMS Collaboration, "Performance of b tagging at $\sqrt{s}$ = 8 TeV in multijet, ttbar and boosted topology events", CMS Physics Analysis Summary CMS-PAS-BTV-13-001, 2013.

[68] J. M. Campbell and R. K. Ellis, "MCFM for the Tevatron and the LHC", *Nucl. Phys. Proc. Suppl.* **205** (2010) 10, doi:10.1016/j.nuclphysbps.2010.08.011, arXiv:1007.3492.

[69] CMS Collaboration, "Measurement of the inclusive W and Z production cross sections in pp collisions at $\sqrt{s} = 7$ TeV", *JHEP* **10** (2011) 132, doi:10.1007/JHEP10(2011)132, arXiv:1107.4789.

[70] S. Alekhin et al., "The PDF4LHC Working Group Interim Report", (2011). arXiv:1101.0536.

[71] M. Botje et al., "The PDF4LHC Working Group Interim Recommendations", (2011). arXiv:1101.0538.

[72] NNPDF Collaboration, "Parton distributions with LHC data", *Nucl. Phys. B* **867** (2013) 244, doi:10.1016/j.nuclphysb.2012.10.003, arXiv:1207.1303.

[73] P. M. Nadolsky et al., "Implications of CTEQ global analysis for collider observables", *Phys. Rev. D* **78** (2008) 013004, doi:10.1103/PhysRevD.78.013004, arXiv:0802.0007.

[74] A. D. Martin, W. J. Stirling, R. S. Thorne, and G. Watt, "Parton distributions for the LHC", *Eur. Phys. J. C* **63** (2009) 189, doi:10.1140/epjc/s10052-009-1072-5, arXiv:0901.0002.

[75] P. Nason and G. Zanderighi, "W^+W^- , WZ and ZZ production in the POWHEG-BOX-V2", *Eur. Phys. J. C* **74** (2014) 2702, doi:10.1140/epjc/s10052-013-2702-5, arXiv:1311.1365.

[76] T. Gleisberg et al., "Event generation with SHERPA 1.1", *JHEP* **02** (2009) 007, doi:10.1088/1126-6708/2009/02/007, arXiv:0811.4622.

[77] A. L. Read, "Presentation of search results: the CL_s technique", *J. Phys. G* **28** (2002) 2693, doi:10.1088/0954-3899/28/10/313.

[78] T. Junk, "Confidence level computation for combining searches with small statistics", *Nucl. Instrum. Meth. A* **434** (1999) 435, doi:10.1016/S0168-9002(99)00498-2, arXiv:hep-ex/9902006.

[79] G. Cowan, K. Cranmer, E. Gross, and O. Vitells, "Asymptotic formulae for likelihood-based tests of new physics", *Eur. Phys. J. C* **71** (2011) 1554, doi:10.1140/epjc/s10052-011-1554-0, arXiv:1007.1727. [Erratum: doi:10.1140/epjc/s10052-013-2501-z].

[80] ATLAS and CMS Collaborations, LHC Higgs Combination Group, "Procedure for the LHC Higgs boson search combination in Summer 2011", Technical Report ATL-PHYS-PUB-2011-11, CMS NOTE 2011/005, 2011.

[81] Planck Collaboration, "Planck 2013 results. XVI. Cosmological parameters", *Astron. Astrophys.* **571** (2014) A16, doi:10.1051/0004-6361/201321591, arXiv:1303.5076.

[82] M. Backović, K. Kong, and M. McCaskey, "MadDM v.1.0: Computation of dark matter relic abundance using MadGraph5", *Physics of the Dark Universe* **5** (2014) 18, doi:10.1016/j.dark.2014.04.001, arXiv:1308.4955.

[83] Y. Bai, P. J. Fox, and R. Harnik, "The Tevatron at the frontier of dark matter direct detection", *JHEP* **12** (2010) 048, doi:10.1007/JHEP12(2010)048, arXiv:1005.3797.

[84] A. Friedland, M. L. Graesser, I. M. Shoemaker, and L. Vecchi, "Probing nonstandard standard model backgrounds with LHC monojets", *Phys. Lett. B* **714** (2012) 267, doi:10.1016/j.physletb.2012.06.078, arXiv:1111.5331.

[85] O. Buchmueller, M. J. Dolan, and C. McCabe, "Beyond effective field theory for dark matter searches at the LHC", *JHEP* **01** (2014) 025, doi:10.1007/JHEP01(2014)025, arXiv:1308.6799.

[86] P. J. Fox, R. Harnik, J. Kopp, and Y. Tsai, "Missing energy signatures of dark matter at the LHC", *Phys. Rev. D* **85** (2012) 056011, doi:10.1103/PhysRevD.85.056011, arXiv:1109.4398.

[87] J. Goodman and W. Shepherd, "LHC Bounds on UV-Complete Models of Dark Matter", (2011). arXiv:1111.2359.

[88] I. M. Shoemaker and L. Vecchi, "Unitarity and monojet bounds on models for DAMA, CoGeNT, and CRESST-II", *Phys. Rev. D* **86** (2012) 015023, doi:10.1103/PhysRevD.86.015023, arXiv:1112.5457.

[89] G. Busoni, A. De Simone, E. Morgante, and A. Riotto, "On the validity of the effective field theory for dark matter searches at the LHC", *Phys. Lett. B* **728** (2014) 412, doi:10.1016/j.physletb.2013.11.069, arXiv:1307.2253.

[90] G. Busoni et al., "On the validity of the effective field theory for dark matter searches at the LHC, part II: complete analysis for the *s*-channel", *JCAP* **06** (2014) 060, doi:10.1088/1475-7516/2014/06/060, arXiv:1402.1275.

[91] G. Busoni et al., "On the Validity of the Effective Field Theory for Dark Matter Searches at the LHC Part III: Analysis for the *t*-channel", *JCAP* **09** (2014) 022, doi:10.1088/1475-7516/2014/09/022, arXiv:1405.3101.

[92] S. Malik et al., "Interplay and Characterization of Dark Matter Searches at Colliders and in Direct Detection Experiments", *Physics of the Dark Universe* **9–10** (2015) 51, doi:10.1016/j.dark.2015.03.003, arXiv:1409.4075.

[93] J. Abdallah et al., "Simplified models for dark matter searches at the LHC", *Physics of the Dark Universe* **9** (2015) 8, doi:10.1016/j.dark.2015.08.001, arXiv:1506.03116.

[94] D. Abercrombie et al., "Dark Matter Benchmark Models for Early LHC Run-2 Searches: Report of the ATLAS/CMS Dark Matter Forum", (2015). arXiv:1507.00966.

[95] G. Belanger, F. Boudjema, A. Pukhov, and A. Semenov, "Dark matter direct detection rate in a generic model with micrOMEGAs 2.2", *Comput. Phys. Commun.* **180** (2009) 747, doi:10.1016/j.cpc.2008.11.019, arXiv:0803.2360.

[96] CMS Collaboration, "Search for invisible decays of Higgs bosons in the vector boson fusion and associated ZH production modes", *Eur. Phys. J. C* **74** (2014) 2980, doi:10.1140/epjc/s10052-014-2980-6, arXiv:1404.1344.

[97] A. Djouadi, O. Lebedev, Y. Mambrini, and J. Quevillon, "Implications of LHC searches for Higgs–portal dark matter", *Phys. Lett. B* **709** (2012) 65, doi:10.1016/j.physletb.2012.01.062, arXiv:1112.3299.

[98] A. Djouadi, A. Falkowski, Y. Mambrini, and J. Quevillon, "Direct detection of Higgs-portal dark matter at the LHC", *Eur. Phys. J. C* **73** (2013) 2455, doi:10.1140/epjc/s10052-013-2455-1, arXiv:1205.3169.

[99] R. D. Young and A. W. Thomas, "Octet baryon masses and sigma terms from an SU(3) chiral extrapolation", *Phys. Rev. D* **81** (2010) 014503, doi:10.1103/PhysRevD.81.014503, arXiv:0901.3310.

[100] MILC Collaboration, "The Strange Quark Condensate in the Nucleon in 2+1 Flavor QCD", *Phys. Rev. Lett.* **103** (2009) 122002, doi:10.1103/PhysRevLett.103.122002, arXiv:0905.2432.

[101] PICO Collaboration, "Dark Matter Search Results from the PICO-2L C_3F_8 Bubble Chamber", *Phys. Rev. Lett.* **114** (2015) 231302, doi:10.1103/PhysRevLett.114.231302, arXiv:1503.00008.

[102] XENON100 Collaboration, "Limits on Spin-Dependent WIMP-Nucleon Cross Sections from 225 Live Days of XENON100 Data", *Phys. Rev. Lett.* **111** (2013) 021301, doi:10.1103/PhysRevLett.111.021301, arXiv:1301.6620.

[103] HESS Collaboration, "Constraints on an Annihilation Signal from a Core of Constant Dark Matter Density around the Milky Way Center with H.E.S.S.", *Phys. Rev. Lett.* **114** (2015) 081301, doi:10.1103/PhysRevLett.114.081301, arXiv:1502.03244.

[104] Fermi-LAT Collaboration, "Dark matter constraints from observations of 25 Milky Way satellite galaxies with the Fermi Large Area telescope", *Phys. Rev. D* **89** (2014) 042001, doi:10.1103/PhysRevD.89.042001, arXiv:1310.0828.

A The CMS Collaboration

Yerevan Physics Institute, Yerevan, Armenia
V. Khachatryan, A.M. Sirunyan, A. Tumasyan

Institut für Hochenergiephysik der OeAW, Wien, Austria
W. Adam, E. Asilar, T. Bergauer, J. Brandstetter, E. Brondolin, M. Dragicevic, J. Erö, M. Flechl, M. Friedl, R. Frühwirth[1], V.M. Ghete, C. Hartl, N. Hörmann, J. Hrubec, M. Jeitler[1], V. Knünz, A. König, M. Krammer[1], I. Krätschmer, D. Liko, T. Matsushita, I. Mikulec, D. Rabady[2], B. Rahbaran, H. Rohringer, J. Schieck[1], R. Schöfbeck, J. Strauss, W. Treberer-Treberspurg, W. Waltenberger, C.-E. Wulz[1]

National Centre for Particle and High Energy Physics, Minsk, Belarus
V. Mossolov, N. Shumeiko, J. Suarez Gonzalez

Universiteit Antwerpen, Antwerpen, Belgium
S. Alderweireldt, T. Cornelis, E.A. De Wolf, X. Janssen, A. Knutsson, J. Lauwers, S. Luyckx, M. Van De Klundert, H. Van Haevermaet, P. Van Mechelen, N. Van Remortel, A. Van Spilbeeck

Vrije Universiteit Brussel, Brussel, Belgium
S. Abu Zeid, F. Blekman, J. D'Hondt, N. Daci, I. De Bruyn, K. Deroover, N. Heracleous, J. Keaveney, S. Lowette, L. Moreels, A. Olbrechts, Q. Python, D. Strom, S. Tavernier, W. Van Doninck, P. Van Mulders, G.P. Van Onsem, I. Van Parijs

Université Libre de Bruxelles, Bruxelles, Belgium
P. Barria, H. Brun, C. Caillol, B. Clerbaux, G. De Lentdecker, G. Fasanella, L. Favart, A. Grebenyuk, G. Karapostoli, T. Lenzi, A. Léonard, T. Maerschalk, A. Marinov, L. Perniè, A. Randle-conde, T. Seva, C. Vander Velde, P. Vanlaer, R. Yonamine, F. Zenoni, F. Zhang[3]

Ghent University, Ghent, Belgium
K. Beernaert, L. Benucci, A. Cimmino, S. Crucy, D. Dobur, A. Fagot, G. Garcia, M. Gul, J. Mccartin, A.A. Ocampo Rios, D. Poyraz, D. Ryckbosch, S. Salva, M. Sigamani, M. Tytgat, W. Van Driessche, E. Yazgan, N. Zaganidis

Université Catholique de Louvain, Louvain-la-Neuve, Belgium
S. Basegmez, C. Beluffi[4], O. Bondu, S. Brochet, G. Bruno, A. Caudron, L. Ceard, G.G. Da Silveira, C. Delaere, D. Favart, L. Forthomme, A. Giammanco[5], J. Hollar, A. Jafari, P. Jez, M. Komm, V. Lemaitre, A. Mertens, M. Musich, C. Nuttens, L. Perrini, A. Pin, K. Piotrzkowski, A. Popov[6], L. Quertenmont, M. Selvaggi, M. Vidal Marono

Université de Mons, Mons, Belgium
N. Beliy, G.H. Hammad

Centro Brasileiro de Pesquisas Fisicas, Rio de Janeiro, Brazil
W.L. Aldá Júnior, F.L. Alves, G.A. Alves, L. Brito, M. Correa Martins Junior, M. Hamer, C. Hensel, C. Mora Herrera, A. Moraes, M.E. Pol, P. Rebello Teles

Universidade do Estado do Rio de Janeiro, Rio de Janeiro, Brazil
E. Belchior Batista Das Chagas, W. Carvalho, J. Chinellato[7], A. Custódio, E.M. Da Costa, D. De Jesus Damiao, C. De Oliveira Martins, S. Fonseca De Souza, L.M. Huertas Guativa, H. Malbouisson, D. Matos Figueiredo, L. Mundim, H. Nogima, W.L. Prado Da Silva, A. Santoro, A. Sznajder, E.J. Tonelli Manganote[7], A. Vilela Pereira

Universidade Estadual Paulista [a], Universidade Federal do ABC [b], São Paulo, Brazil
S. Ahuja[a], C.A. Bernardes[b], A. De Souza Santos[b], S. Dogra[a], T.R. Fernandez Perez Tomei[a],

E.M. Gregores[b], P.G. Mercadante[b], C.S. Moon[a,8], S.F. Novaes[a], Sandra S. Padula[a], D. Romero Abad, J.C. Ruiz Vargas

Institute for Nuclear Research and Nuclear Energy, Sofia, Bulgaria
A. Aleksandrov, R. Hadjiiska, P. Iaydjiev, M. Rodozov, S. Stoykova, G. Sultanov, M. Vutova

University of Sofia, Sofia, Bulgaria
A. Dimitrov, I. Glushkov, L. Litov, B. Pavlov, P. Petkov

Institute of High Energy Physics, Beijing, China
M. Ahmad, J.G. Bian, G.M. Chen, H.S. Chen, M. Chen, T. Cheng, R. Du, C.H. Jiang, R. Plestina[9], F. Romeo, S.M. Shaheen, A. Spiezia, J. Tao, C. Wang, Z. Wang, H. Zhang

State Key Laboratory of Nuclear Physics and Technology, Peking University, Beijing, China
C. Asawatangtrakuldee, Y. Ban, Q. Li, S. Liu, Y. Mao, S.J. Qian, D. Wang, Z. Xu

Universidad de Los Andes, Bogota, Colombia
C. Avila, A. Cabrera, L.F. Chaparro Sierra, C. Florez, J.P. Gomez, B. Gomez Moreno, J.C. Sanabria

University of Split, Faculty of Electrical Engineering, Mechanical Engineering and Naval Architecture, Split, Croatia
N. Godinovic, D. Lelas, I. Puljak, P.M. Ribeiro Cipriano

University of Split, Faculty of Science, Split, Croatia
Z. Antunovic, M. Kovac

Institute Rudjer Boskovic, Zagreb, Croatia
V. Brigljevic, K. Kadija, J. Luetic, S. Micanovic, L. Sudic

University of Cyprus, Nicosia, Cyprus
A. Attikis, G. Mavromanolakis, J. Mousa, C. Nicolaou, F. Ptochos, P.A. Razis, H. Rykaczewski

Charles University, Prague, Czech Republic
M. Bodlak, M. Finger[10], M. Finger Jr.[10]

Academy of Scientific Research and Technology of the Arab Republic of Egypt, Egyptian Network of High Energy Physics, Cairo, Egypt
Y. Assran[11], S. Elgammal[12], A. Ellithi Kamel[13,13], M.A. Mahmoud[14,14], Y. Mohammed[14]

National Institute of Chemical Physics and Biophysics, Tallinn, Estonia
B. Calpas, M. Kadastik, M. Murumaa, M. Raidal, A. Tiko, C. Veelken

Department of Physics, University of Helsinki, Helsinki, Finland
P. Eerola, J. Pekkanen, M. Voutilainen

Helsinki Institute of Physics, Helsinki, Finland
J. Härkönen, V. Karimäki, R. Kinnunen, T. Lampén, K. Lassila-Perini, S. Lehti, T. Lindén, P. Luukka, T. Mäenpää, T. Peltola, E. Tuominen, J. Tuominiemi, E. Tuovinen, L. Wendland

Lappeenranta University of Technology, Lappeenranta, Finland
J. Talvitie, T. Tuuva

DSM/IRFU, CEA/Saclay, Gif-sur-Yvette, France
M. Besancon, F. Couderc, M. Dejardin, D. Denegri, B. Fabbro, J.L. Faure, C. Favaro, F. Ferri, S. Ganjour, A. Givernaud, P. Gras, G. Hamel de Monchenault, P. Jarry, E. Locci, M. Machet, J. Malcles, J. Rander, A. Rosowsky, M. Titov, A. Zghiche

Laboratoire Leprince-Ringuet, Ecole Polytechnique, IN2P3-CNRS, Palaiseau, France
I. Antropov, S. Baffioni, F. Beaudette, P. Busson, L. Cadamuro, E. Chapon, C. Charlot, T. Dahms, O. Davignon, N. Filipovic, R. Granier de Cassagnac, M. Jo, S. Lisniak, L. Mastrolorenzo, P. Miné, I.N. Naranjo, M. Nguyen, C. Ochando, G. Ortona, P. Paganini, P. Pigard, S. Regnard, R. Salerno, J.B. Sauvan, Y. Sirois, T. Strebler, Y. Yilmaz, A. Zabi

Institut Pluridisciplinaire Hubert Curien, Université de Strasbourg, Université de Haute Alsace Mulhouse, CNRS/IN2P3, Strasbourg, France
J.-L. Agram[15], J. Andrea, A. Aubin, D. Bloch, J.-M. Brom, M. Buttignol, E.C. Chabert, N. Chanon, C. Collard, E. Conte[15], X. Coubez, J.-C. Fontaine[15], D. Gelé, U. Goerlach, C. Goetzmann, A.-C. Le Bihan, J.A. Merlin[2], K. Skovpen, P. Van Hove

Centre de Calcul de l'Institut National de Physique Nucleaire et de Physique des Particules, CNRS/IN2P3, Villeurbanne, France
S. Gadrat

Université de Lyon, Université Claude Bernard Lyon 1, CNRS-IN2P3, Institut de Physique Nucléaire de Lyon, Villeurbanne, France
S. Beauceron, C. Bernet, G. Boudoul, E. Bouvier, C.A. Carrillo Montoya, R. Chierici, D. Contardo, B. Courbon, P. Depasse, H. El Mamouni, J. Fan, J. Fay, S. Gascon, M. Gouzevitch, B. Ille, F. Lagarde, I.B. Laktineh, M. Lethuillier, L. Mirabito, A.L. Pequegnot, S. Perries, J.D. Ruiz Alvarez, D. Sabes, L. Sgandurra, V. Sordini, M. Vander Donckt, P. Verdier, S. Viret

Georgian Technical University, Tbilisi, Georgia
T. Toriashvili[16]

Tbilisi State University, Tbilisi, Georgia
Z. Tsamalaidze[10]

RWTH Aachen University, I. Physikalisches Institut, Aachen, Germany
C. Autermann, S. Beranek, M. Edelhoff, L. Feld, A. Heister, M.K. Kiesel, K. Klein, M. Lipinski, A. Ostapchuk, M. Preuten, F. Raupach, S. Schael, J.F. Schulte, T. Verlage, H. Weber, B. Wittmer, V. Zhukov[6]

RWTH Aachen University, III. Physikalisches Institut A, Aachen, Germany
M. Ata, M. Brodski, E. Dietz-Laursonn, D. Duchardt, M. Endres, M. Erdmann, S. Erdweg, T. Esch, R. Fischer, A. Güth, T. Hebbeker, C. Heidemann, K. Hoepfner, S. Knutzen, P. Kreuzer, M. Merschmeyer, A. Meyer, P. Millet, M. Olschewski, K. Padeken, P. Papacz, T. Pook, M. Radziej, H. Reithler, M. Rieger, F. Scheuch, L. Sonnenschein, D. Teyssier, S. Thüer

RWTH Aachen University, III. Physikalisches Institut B, Aachen, Germany
V. Cherepanov, Y. Erdogan, G. Flügge, H. Geenen, M. Geisler, F. Hoehle, B. Kargoll, T. Kress, Y. Kuessel, A. Künsken, J. Lingemann, A. Nehrkorn, A. Nowack, I.M. Nugent, C. Pistone, O. Pooth, A. Stahl

Deutsches Elektronen-Synchrotron, Hamburg, Germany
M. Aldaya Martin, I. Asin, N. Bartosik, O. Behnke, U. Behrens, A.J. Bell, K. Borras[17], A. Burgmeier, A. Campbell, S. Choudhury[18], F. Costanza, C. Diez Pardos, G. Dolinska, S. Dooling, T. Dorland, G. Eckerlin, D. Eckstein, T. Eichhorn, G. Flucke, E. Gallo[19], J. Garay Garcia, A. Geiser, A. Gizhko, P. Gunnellini, J. Hauk, M. Hempel[20], H. Jung, A. Kalogeropoulos, O. Karacheban[20], M. Kasemann, P. Katsas, J. Kieseler, C. Kleinwort, I. Korol, W. Lange, J. Leonard, K. Lipka, A. Lobanov, W. Lohmann[20], R. Mankel, I. Marfin[20], I.-A. Melzer-Pellmann, A.B. Meyer, G. Mittag, J. Mnich, A. Mussgiller, S. Naumann-Emme, A. Nayak, E. Ntomari,

H. Perrey, D. Pitzl, R. Placakyte, A. Raspereza, B. Roland, M.Ö. Sahin, P. Saxena, T. Schoerner-Sadenius, M. Schröder, C. Seitz, S. Spannagel, K.D. Trippkewitz, R. Walsh, C. Wissing

University of Hamburg, Hamburg, Germany
V. Blobel, M. Centis Vignali, A.R. Draeger, J. Erfle, E. Garutti, K. Goebel, D. Gonzalez, M. Görner, J. Haller, M. Hoffmann, R.S. Höing, A. Junkes, R. Klanner, R. Kogler, N. Kovalchuk, T. Lapsien, T. Lenz, I. Marchesini, D. Marconi, M. Meyer, D. Nowatschin, J. Ott, F. Pantaleo[2], T. Peiffer, A. Perieanu, N. Pietsch, J. Poehlsen, D. Rathjens, C. Sander, C. Scharf, H. Schettler, P. Schleper, E. Schlieckau, A. Schmidt, J. Schwandt, V. Sola, H. Stadie, G. Steinbrück, H. Tholen, D. Troendle, E. Usai, L. Vanelderen, A. Vanhoefer, B. Vormwald

Institut für Experimentelle Kernphysik, Karlsruhe, Germany
M. Akbiyik, C. Barth, C. Baus, J. Berger, C. Böser, E. Butz, T. Chwalek, F. Colombo, W. De Boer, A. Descroix, A. Dierlamm, S. Fink, F. Frensch, R. Friese, M. Giffels, A. Gilbert, D. Haitz, F. Hartmann[2], S.M. Heindl, U. Husemann, I. Katkov[6], A. Kornmayer[2], P. Lobelle Pardo, B. Maier, H. Mildner, M.U. Mozer, T. Müller, Th. Müller, M. Plagge, G. Quast, K. Rabbertz, S. Röcker, F. Roscher, G. Sieber, H.J. Simonis, F.M. Stober, R. Ulrich, J. Wagner-Kuhr, S. Wayand, M. Weber, T. Weiler, C. Wöhrmann, R. Wolf

Institute of Nuclear and Particle Physics (INPP), NCSR Demokritos, Aghia Paraskevi, Greece
G. Anagnostou, G. Daskalakis, T. Geralis, V.A. Giakoumopoulou, A. Kyriakis, D. Loukas, A. Psallidas, I. Topsis-Giotis

University of Athens, Athens, Greece
A. Agapitos, S. Kesisoglou, A. Panagiotou, N. Saoulidou, E. Tziaferi

University of Ioánnina, Ioánnina, Greece
I. Evangelou, G. Flouris, C. Foudas, P. Kokkas, N. Loukas, N. Manthos, I. Papadopoulos, E. Paradas, J. Strologas

Wigner Research Centre for Physics, Budapest, Hungary
G. Bencze, C. Hajdu, A. Hazi, P. Hidas, D. Horvath[21], F. Sikler, V. Veszpremi, G. Vesztergombi[22], A.J. Zsigmond

Institute of Nuclear Research ATOMKI, Debrecen, Hungary
N. Beni, S. Czellar, J. Karancsi[23], J. Molnar, Z. Szillasi[2]

University of Debrecen, Debrecen, Hungary
M. Bartók[24], A. Makovec, P. Raics, Z.L. Trocsanyi, B. Ujvari

National Institute of Science Education and Research, Bhubaneswar, India
P. Mal, K. Mandal, D.K. Sahoo, N. Sahoo, S.K. Swain

Panjab University, Chandigarh, India
S. Bansal, S.B. Beri, V. Bhatnagar, R. Chawla, R. Gupta, U.Bhawandeep, A.K. Kalsi, A. Kaur, M. Kaur, R. Kumar, A. Mehta, M. Mittal, J.B. Singh, G. Walia

University of Delhi, Delhi, India
Ashok Kumar, A. Bhardwaj, B.C. Choudhary, R.B. Garg, A. Kumar, S. Malhotra, M. Naimuddin, N. Nishu, K. Ranjan, R. Sharma, V. Sharma

Saha Institute of Nuclear Physics, Kolkata, India
S. Bhattacharya, K. Chatterjee, S. Dey, S. Dutta, Sa. Jain, N. Majumdar, A. Modak, K. Mondal, S. Mukherjee, S. Mukhopadhyay, A. Roy, D. Roy, S. Roy Chowdhury, S. Sarkar, M. Sharan

Bhabha Atomic Research Centre, Mumbai, India
A. Abdulsalam, R. Chudasama, D. Dutta, V. Jha, V. Kumar, A.K. Mohanty[2], L.M. Pant, P. Shukla, A. Topkar

Tata Institute of Fundamental Research, Mumbai, India
T. Aziz, S. Banerjee, S. Bhowmik[25], R.M. Chatterjee, R.K. Dewanjee, S. Dugad, S. Ganguly, S. Ghosh, M. Guchait, A. Gurtu[26], G. Kole, S. Kumar, B. Mahakud, M. Maity[25], G. Majumder, K. Mazumdar, S. Mitra, G.B. Mohanty, B. Parida, T. Sarkar[25], N. Sur, B. Sutar, N. Wickramage[27]

Indian Institute of Science Education and Research (IISER), Pune, India
S. Chauhan, S. Dube, K. Kothekar, S. Sharma

Institute for Research in Fundamental Sciences (IPM), Tehran, Iran
H. Bakhshiansohi, H. Behnamian, S.M. Etesami[28], A. Fahim[29], R. Goldouzian, M. Khakzad, M. Mohammadi Najafabadi, M. Naseri, S. Paktinat Mehdiabadi, F. Rezaei Hosseinabadi, B. Safarzadeh[30], M. Zeinali

University College Dublin, Dublin, Ireland
M. Felcini, M. Grunewald

INFN Sezione di Bari [a], Università di Bari [b], Politecnico di Bari [c], Bari, Italy
M. Abbrescia[a,b], C. Calabria[a,b], C. Caputo[a,b], A. Colaleo[a], D. Creanza[a,c], L. Cristella[a,b], N. De Filippis[a,c], M. De Palma[a,b], L. Fiore[a], G. Iaselli[a,c], G. Maggi[a,c], M. Maggi[a], G. Miniello[a,b], S. My[a,c], S. Nuzzo[a,b], A. Pompili[a,b], G. Pugliese[a,c], R. Radogna[a,b], A. Ranieri[a], G. Selvaggi[a,b], L. Silvestris[a,2], R. Venditti[a,b], P. Verwilligen[a]

INFN Sezione di Bologna [a], Università di Bologna [b], Bologna, Italy
G. Abbiendi[a], C. Battilana[2], A.C. Benvenuti[a], D. Bonacorsi[a,b], S. Braibant-Giacomelli[a,b], L. Brigliadori[a,b], R. Campanini[a,b], P. Capiluppi[a,b], A. Castro[a,b], F.R. Cavallo[a], S.S. Chhibra[a,b], G. Codispoti[a,b], M. Cuffiani[a,b], G.M. Dallavalle[a], F. Fabbri[a], A. Fanfani[a,b], D. Fasanella[a,b], P. Giacomelli[a], C. Grandi[a], L. Guiducci[a,b], S. Marcellini[a], G. Masetti[a], A. Montanari[a], F.L. Navarria[a,b], A. Perrotta[a], A.M. Rossi[a,b], T. Rovelli[a,b], G.P. Siroli[a,b], N. Tosi[a,b,2], R. Travaglini[a,b]

INFN Sezione di Catania [a], Università di Catania [b], Catania, Italy
G. Cappello[a], M. Chiorboli[a,b], S. Costa[a,b], A. Di Mattia[a], F. Giordano[a,b], R. Potenza[a,b], A. Tricomi[a,b], C. Tuve[a,b]

INFN Sezione di Firenze [a], Università di Firenze [b], Firenze, Italy
G. Barbagli[a], V. Ciulli[a,b], C. Civinini[a], R. D'Alessandro[a,b], E. Focardi[a,b], S. Gonzi[a,b], V. Gori[a,b], P. Lenzi[a,b], M. Meschini[a], S. Paoletti[a], G. Sguazzoni[a], A. Tropiano[a,b], L. Viliani[a,b,2]

INFN Laboratori Nazionali di Frascati, Frascati, Italy
L. Benussi, S. Bianco, F. Fabbri, D. Piccolo, F. Primavera[2]

INFN Sezione di Genova [a], Università di Genova [b], Genova, Italy
V. Calvelli[a,b], F. Ferro[a], M. Lo Vetere[a,b], M.R. Monge[a,b], E. Robutti[a], S. Tosi[a,b]

INFN Sezione di Milano-Bicocca [a], Università di Milano-Bicocca [b], Milano, Italy
L. Brianza, M.E. Dinardo[a,b], S. Fiorendi[a,b], S. Gennai[a], R. Gerosa[a,b], A. Ghezzi[a,b], P. Govoni[a,b], S. Malvezzi[a], R.A. Manzoni[a,b,2], B. Marzocchi[a,b], D. Menasce[a], L. Moroni[a], M. Paganoni[a,b], D. Pedrini[a], S. Ragazzi[a,b], N. Redaelli[a], T. Tabarelli de Fatis[a,b]

INFN Sezione di Napoli [a], Università di Napoli 'Federico II' [b], Napoli, Italy, Università della Basilicata [c], Potenza, Italy, Università G. Marconi [d], Roma, Italy
S. Buontempo[a], N. Cavallo[a,c], S. Di Guida[a,d,2], M. Esposito[a,b], F. Fabozzi[a,c], A.O.M. Iorio[a,b], G. Lanza[a], L. Lista[a], S. Meola[a,d,2], M. Merola[a], P. Paolucci[a,2], C. Sciacca[a,b], F. Thyssen

INFN Sezione di Padova [a], Università di Padova [b], Padova, Italy, Università di Trento [c], Trento, Italy
P. Azzi[a,2], N. Bacchetta[a], L. Benato[a,b], D. Bisello[a,b], A. Boletti[a,b], A. Branca[a,b], R. Carlin[a,b], P. Checchia[a], M. Dall'Osso[a,b,2], T. Dorigo[a], U. Dosselli[a], F. Gasparini[a,b], U. Gasparini[a,b], A. Gozzelino[a], K. Kanishchev[a,c], S. Lacaprara[a], M. Margoni[a,b], A.T. Meneguzzo[a,b], M. Passaseo[a], J. Pazzini[a,b,2], N. Pozzobon[a,b], P. Ronchese[a,b], F. Simonetto[a,b], E. Torassa[a], M. Tosi[a,b], M. Zanetti, P. Zotto[a,b], A. Zucchetta[a,b,2], G. Zumerle[a,b]

INFN Sezione di Pavia [a], Università di Pavia [b], Pavia, Italy
A. Braghieri[a], A. Magnani[a], P. Montagna[a,b], S.P. Ratti[a,b], V. Re[a], C. Riccardi[a,b], P. Salvini[a], I. Vai[a], P. Vitulo[a,b]

INFN Sezione di Perugia [a], Università di Perugia [b], Perugia, Italy
L. Alunni Solestizi[a,b], G.M. Bilei[a], D. Ciangottini[a,b,2], L. Fanò[a,b], P. Lariccia[a,b], G. Mantovani[a,b], M. Menichelli[a], A. Saha[a], A. Santocchia[a,b]

INFN Sezione di Pisa [a], Università di Pisa [b], Scuola Normale Superiore di Pisa [c], Pisa, Italy
K. Androsov[a,31], P. Azzurri[a,2], G. Bagliesi[a], J. Bernardini[a], T. Boccali[a], R. Castaldi[a], M.A. Ciocci[a,31], R. Dell'Orso[a], S. Donato[a,c,2], G. Fedi, L. Foà[a,c†], A. Giassi[a], M.T. Grippo[a,31], F. Ligabue[a,c], T. Lomtadze[a], L. Martini[a,b], A. Messineo[a,b], F. Palla[a], A. Rizzi[a,b], A. Savoy-Navarro[a,32], A.T. Serban[a], P. Spagnolo[a], R. Tenchini[a], G. Tonelli[a,b], A. Venturi[a], P.G. Verdini[a]

INFN Sezione di Roma [a], Università di Roma [b], Roma, Italy
L. Barone[a,b], F. Cavallari[a], G. D'imperio[a,b,2], D. Del Re[a,b,2], M. Diemoz[a], S. Gelli[a,b], C. Jorda[a], E. Longo[a,b], F. Margaroli[a,b], P. Meridiani[a], G. Organtini[a,b], R. Paramatti[a], F. Preiato[a,b], S. Rahatlou[a,b], C. Rovelli[a], F. Santanastasio[a,b], P. Traczyk[a,b,2]

INFN Sezione di Torino [a], Università di Torino [b], Torino, Italy, Università del Piemonte Orientale [c], Novara, Italy
N. Amapane[a,b], R. Arcidiacono[a,c,2], S. Argiro[a,b], M. Arneodo[a,c], R. Bellan[a,b], C. Biino[a], N. Cartiglia[a], M. Costa[a,b], R. Covarelli[a,b], A. Degano[a,b], N. Demaria[a], L. Finco[a,b,2], C. Mariotti[a], S. Maselli[a], G. Mazza[a], E. Migliore[a,b], V. Monaco[a,b], E. Monteil[a,b], M.M. Obertino[a,b], L. Pacher[a,b], N. Pastrone[a], M. Pelliccioni[a], G.L. Pinna Angioni[a,b], F. Ravera[a,b], A. Romero[a,b], M. Ruspa[a,c], R. Sacchi[a,b], A. Solano[a,b], A. Staiano[a]

INFN Sezione di Trieste [a], Università di Trieste [b], Trieste, Italy
S. Belforte[a], V. Candelise[a,b,2], M. Casarsa[a], F. Cossutti[a], G. Della Ricca[a,b], B. Gobbo[a], C. La Licata[a,b], M. Marone[a,b], A. Schizzi[a,b], A. Zanetti[a]

Kangwon National University, Chunchon, Korea
A. Kropivnitskaya, S.K. Nam

Kyungpook National University, Daegu, Korea
D.H. Kim, G.N. Kim, M.S. Kim, D.J. Kong, S. Lee, Y.D. Oh, A. Sakharov, D.C. Son

Chonbuk National University, Jeonju, Korea
J.A. Brochero Cifuentes, H. Kim, T.J. Kim

Chonnam National University, Institute for Universe and Elementary Particles, Kwangju, Korea
S. Song

Korea University, Seoul, Korea
S. Choi, Y. Go, D. Gyun, B. Hong, H. Kim, Y. Kim, B. Lee, K. Lee, K.S. Lee, S. Lee, S.K. Park, Y. Roh

Seoul National University, Seoul, Korea
H.D. Yoo

University of Seoul, Seoul, Korea
M. Choi, H. Kim, J.H. Kim, J.S.H. Lee, I.C. Park, G. Ryu, M.S. Ryu

Sungkyunkwan University, Suwon, Korea
Y. Choi, J. Goh, D. Kim, E. Kwon, J. Lee, I. Yu

Vilnius University, Vilnius, Lithuania
V. Dudenas, A. Juodagalvis, J. Vaitkus

National Centre for Particle Physics, Universiti Malaya, Kuala Lumpur, Malaysia
I. Ahmed, Z.A. Ibrahim, J.R. Komaragiri, M.A.B. Md Ali[33], F. Mohamad Idris[34], W.A.T. Wan Abdullah, M.N. Yusli

Centro de Investigacion y de Estudios Avanzados del IPN, Mexico City, Mexico
E. Casimiro Linares, H. Castilla-Valdez, E. De La Cruz-Burelo, I. Heredia-De La Cruz[35], A. Hernandez-Almada, R. Lopez-Fernandez, A. Sanchez-Hernandez

Universidad Iberoamericana, Mexico City, Mexico
S. Carrillo Moreno, F. Vazquez Valencia

Benemerita Universidad Autonoma de Puebla, Puebla, Mexico
I. Pedraza, H.A. Salazar Ibarguen

Universidad Autónoma de San Luis Potosí, San Luis Potosí, Mexico
A. Morelos Pineda

University of Auckland, Auckland, New Zealand
D. Krofcheck

University of Canterbury, Christchurch, New Zealand
P.H. Butler

National Centre for Physics, Quaid-I-Azam University, Islamabad, Pakistan
A. Ahmad, M. Ahmad, Q. Hassan, H.R. Hoorani, W.A. Khan, T. Khurshid, M. Shoaib

National Centre for Nuclear Research, Swierk, Poland
H. Bialkowska, M. Bluj, B. Boimska, T. Frueboes, M. Górski, M. Kazana, K. Nawrocki, K. Romanowska-Rybinska, M. Szleper, P. Zalewski

Institute of Experimental Physics, Faculty of Physics, University of Warsaw, Warsaw, Poland
G. Brona, K. Bunkowski, A. Byszuk[36], K. Doroba, A. Kalinowski, M. Konecki, J. Krolikowski, M. Misiura, M. Olszewski, M. Walczak

Laboratório de Instrumentação e Física Experimental de Partículas, Lisboa, Portugal
P. Bargassa, C. Beirão Da Cruz E Silva, A. Di Francesco, P. Faccioli, P.G. Ferreira Parracho,

M. Gallinaro, N. Leonardo, L. Lloret Iglesias, F. Nguyen, J. Rodrigues Antunes, J. Seixas, O. Toldaiev, D. Vadruccio, J. Varela, P. Vischia

Joint Institute for Nuclear Research, Dubna, Russia
S. Afanasiev, P. Bunin, M. Gavrilenko, I. Golutvin, I. Gorbunov, A. Kamenev, V. Karjavin, V. Konoplyanikov, A. Lanev, A. Malakhov, V. Matveev[37,38], P. Moisenz, V. Palichik, V. Perelygin, S. Shmatov, S. Shulha, N. Skatchkov, V. Smirnov, A. Zarubin

Petersburg Nuclear Physics Institute, Gatchina (St. Petersburg), Russia
V. Golovtsov, Y. Ivanov, V. Kim[39], E. Kuznetsova, P. Levchenko, V. Murzin, V. Oreshkin, I. Smirnov, V. Sulimov, L. Uvarov, S. Vavilov, A. Vorobyev

Institute for Nuclear Research, Moscow, Russia
Yu. Andreev, A. Dermenev, S. Gninenko, N. Golubev, A. Karneyeu, M. Kirsanov, N. Krasnikov, A. Pashenkov, D. Tlisov, A. Toropin

Institute for Theoretical and Experimental Physics, Moscow, Russia
V. Epshteyn, V. Gavrilov, N. Lychkovskaya, V. Popov, I. Pozdnyakov, G. Safronov, A. Spiridonov, E. Vlasov, A. Zhokin

National Research Nuclear University 'Moscow Engineering Physics Institute' (MEPhI), Moscow, Russia
A. Bylinkin

P.N. Lebedev Physical Institute, Moscow, Russia
V. Andreev, M. Azarkin[38], I. Dremin[38], M. Kirakosyan, A. Leonidov[38], G. Mesyats, S.V. Rusakov

Skobeltsyn Institute of Nuclear Physics, Lomonosov Moscow State University, Moscow, Russia
A. Baskakov, A. Belyaev, E. Boos, M. Dubinin[40], L. Dudko, A. Ershov, A. Gribushin, V. Klyukhin, O. Kodolova, I. Lokhtin, I. Myagkov, S. Obraztsov, S. Petrushanko, V. Savrin, A. Snigirev

State Research Center of Russian Federation, Institute for High Energy Physics, Protvino, Russia
I. Azhgirey, I. Bayshev, S. Bitioukov, V. Kachanov, A. Kalinin, D. Konstantinov, V. Krychkine, V. Petrov, R. Ryutin, A. Sobol, L. Tourtchanovitch, S. Troshin, N. Tyurin, A. Uzunian, A. Volkov

University of Belgrade, Faculty of Physics and Vinca Institute of Nuclear Sciences, Belgrade, Serbia
P. Adzic[41], P. Cirkovic, J. Milosevic, V. Rekovic

Centro de Investigaciones Energéticas Medioambientales y Tecnológicas (CIEMAT), Madrid, Spain
J. Alcaraz Maestre, E. Calvo, M. Cerrada, M. Chamizo Llatas, N. Colino, B. De La Cruz, A. Delgado Peris, D. Domínguez Vázquez, A. Escalante Del Valle, C. Fernandez Bedoya, J.P. Fernández Ramos, J. Flix, M.C. Fouz, P. Garcia-Abia, O. Gonzalez Lopez, S. Goy Lopez, J.M. Hernandez, M.I. Josa, E. Navarro De Martino, A. Pérez-Calero Yzquierdo, J. Puerta Pelayo, A. Quintario Olmeda, I. Redondo, L. Romero, J. Santaolalla, M.S. Soares

Universidad Autónoma de Madrid, Madrid, Spain
C. Albajar, J.F. de Trocóniz, M. Missiroli, D. Moran

Universidad de Oviedo, Oviedo, Spain
J. Cuevas, J. Fernandez Menendez, S. Folgueras, I. Gonzalez Caballero, E. Palencia Cortezon, J.M. Vizan Garcia

Instituto de Física de Cantabria (IFCA), CSIC-Universidad de Cantabria, Santander, Spain
I.J. Cabrillo, A. Calderon, J.R. Castiñeiras De Saa, P. De Castro Manzano, M. Fernandez, J. Garcia-Ferrero, G. Gomez, A. Lopez Virto, J. Marco, R. Marco, C. Martinez Rivero, F. Matorras, J. Piedra Gomez, T. Rodrigo, A.Y. Rodríguez-Marrero, A. Ruiz-Jimeno, L. Scodellaro, N. Trevisani, I. Vila, R. Vilar Cortabitarte

CERN, European Organization for Nuclear Research, Geneva, Switzerland
D. Abbaneo, E. Auffray, G. Auzinger, M. Bachtis, P. Baillon, A.H. Ball, D. Barney, A. Benaglia, J. Bendavid, L. Benhabib, J.F. Benitez, G.M. Berruti, P. Bloch, A. Bocci, A. Bonato, C. Botta, H. Breuker, T. Camporesi, R. Castello, G. Cerminara, M. D'Alfonso, D. d'Enterria, A. Dabrowski, V. Daponte, A. David, M. De Gruttola, F. De Guio, A. De Roeck, S. De Visscher, E. Di Marco[42], M. Dobson, M. Dordevic, B. Dorney, T. du Pree, D. Duggan, M. Dünser, N. Dupont, A. Elliott-Peisert, G. Franzoni, J. Fulcher, W. Funk, D. Gigi, K. Gill, D. Giordano, M. Girone, F. Glege, R. Guida, S. Gundacker, M. Guthoff, J. Hammer, P. Harris, J. Hegeman, V. Innocente, P. Janot, H. Kirschenmann, M.J. Kortelainen, K. Kousouris, K. Krajczar, P. Lecoq, C. Lourenço, M.T. Lucchini, N. Magini, L. Malgeri, M. Mannelli, A. Martelli, L. Masetti, F. Meijers, S. Mersi, E. Meschi, F. Moortgat, S. Morovic, M. Mulders, M.V. Nemallapudi, H. Neugebauer, S. Orfanelli[43], L. Orsini, L. Pape, E. Perez, M. Peruzzi, A. Petrilli, G. Petrucciani, A. Pfeiffer, D. Piparo, A. Racz, T. Reis, G. Rolandi[44], M. Rovere, M. Ruan, H. Sakulin, C. Schäfer, C. Schwick, M. Seidel, A. Sharma, P. Silva, M. Simon, P. Sphicas[45], J. Steggemann, B. Stieger, M. Stoye, Y. Takahashi, D. Treille, A. Triossi, A. Tsirou, G.I. Veres[22], N. Wardle, H.K. Wöhri, A. Zagozdzinska[36], W.D. Zeuner

Paul Scherrer Institut, Villigen, Switzerland
W. Bertl, K. Deiters, W. Erdmann, R. Horisberger, Q. Ingram, H.C. Kaestli, D. Kotlinski, U. Langenegger, D. Renker, T. Rohe

Institute for Particle Physics, ETH Zurich, Zurich, Switzerland
F. Bachmair, L. Bäni, L. Bianchini, B. Casal, G. Dissertori, M. Dittmar, M. Donegà, P. Eller, C. Grab, C. Heidegger, D. Hits, J. Hoss, G. Kasieczka, W. Lustermann, B. Mangano, M. Marionneau, P. Martinez Ruiz del Arbol, M. Masciovecchio, D. Meister, F. Micheli, P. Musella, F. Nessi-Tedaldi, F. Pandolfi, J. Pata, F. Pauss, L. Perrozzi, M. Quittnat, M. Rossini, A. Starodumov[46], M. Takahashi, V.R. Tavolaro, K. Theofilatos, R. Wallny

Universität Zürich, Zurich, Switzerland
T.K. Aarrestad, C. Amsler[47], L. Caminada, M.F. Canelli, V. Chiochia, A. De Cosa, C. Galloni, A. Hinzmann, T. Hreus, B. Kilminster, C. Lange, J. Ngadiuba, D. Pinna, P. Robmann, F.J. Ronga, D. Salerno, Y. Yang

National Central University, Chung-Li, Taiwan
M. Cardaci, K.H. Chen, T.H. Doan, Sh. Jain, R. Khurana, M. Konyushikhin, C.M. Kuo, W. Lin, Y.J. Lu, S.S. Yu

National Taiwan University (NTU), Taipei, Taiwan
Arun Kumar, R. Bartek, P. Chang, Y.H. Chang, Y.W. Chang, Y. Chao, K.F. Chen, P.H. Chen, C. Dietz, F. Fiori, U. Grundler, W.-S. Hou, Y. Hsiung, Y.F. Liu, R.-S. Lu, M. Miñano Moya, E. Petrakou, J.f. Tsai, Y.M. Tzeng

Chulalongkorn University, Faculty of Science, Department of Physics, Bangkok, Thailand
B. Asavapibhop, K. Kovitanggoon, G. Singh, N. Srimanobhas, N. Suwonjandee

Cukurova University, Adana, Turkey
A. Adiguzel, S. Cerci[48], Z.S. Demiroglu, C. Dozen, I. Dumanoglu, S. Girgis, G. Gokbulut, Y. Guler, E. Gurpinar, I. Hos, E.E. Kangal[49], A. Kayis Topaksu, G. Onengut[50], K. Ozdemir[51], S. Ozturk[52], A. Polatoz, B. Tali[48], M. Vergili, C. Zorbilmez

Middle East Technical University, Physics Department, Ankara, Turkey
I.V. Akin, B. Bilin, S. Bilmis, B. Isildak[53], G. Karapinar[54], M. Yalvac, M. Zeyrek

Bogazici University, Istanbul, Turkey
E. Gülmez, M. Kaya[55], O. Kaya[56], E.A. Yetkin[57], T. Yetkin[58]

Istanbul Technical University, Istanbul, Turkey
A. Cakir, K. Cankocak, S. Sen[59], F.I. Vardarlı

Institute for Scintillation Materials of National Academy of Science of Ukraine, Kharkov, Ukraine
B. Grynyov

National Scientific Center, Kharkov Institute of Physics and Technology, Kharkov, Ukraine
L. Levchuk, P. Sorokin

University of Bristol, Bristol, United Kingdom
R. Aggleton, F. Ball, L. Beck, J.J. Brooke, E. Clement, D. Cussans, H. Flacher, J. Goldstein, M. Grimes, G.P. Heath, H.F. Heath, J. Jacob, L. Kreczko, C. Lucas, Z. Meng, D.M. Newbold[60], S. Paramesvaran, A. Poll, T. Sakuma, S. Seif El Nasr-storey, S. Senkin, D. Smith, V.J. Smith

Rutherford Appleton Laboratory, Didcot, United Kingdom
K.W. Bell, A. Belyaev[61], C. Brew, R.M. Brown, L. Calligaris, D. Cieri, D.J.A. Cockerill, J.A. Coughlan, K. Harder, S. Harper, E. Olaiya, D. Petyt, C.H. Shepherd-Themistocleous, A. Thea, I.R. Tomalin, T. Williams, S.D. Worm

Imperial College, London, United Kingdom
M. Baber, R. Bainbridge, O. Buchmuller, A. Bundock, D. Burton, S. Casasso, M. Citron, D. Colling, L. Corpe, N. Cripps, P. Dauncey, G. Davies, A. De Wit, M. Della Negra, P. Dunne, A. Elwood, W. Ferguson, D. Futyan, G. Hall, G. Iles, M. Kenzie, R. Lane, R. Lucas[60], L. Lyons, A.-M. Magnan, S. Malik, J. Nash, A. Nikitenko[46], J. Pela, M. Pesaresi, K. Petridis, D.M. Raymond, A. Richards, A. Rose, C. Seez, A. Tapper, K. Uchida, M. Vazquez Acosta[62], T. Virdee, S.C. Zenz

Brunel University, Uxbridge, United Kingdom
J.E. Cole, P.R. Hobson, A. Khan, P. Kyberd, D. Leggat, D. Leslie, I.D. Reid, P. Symonds, L. Teodorescu, M. Turner

Baylor University, Waco, USA
A. Borzou, K. Call, J. Dittmann, K. Hatakeyama, H. Liu, N. Pastika

The University of Alabama, Tuscaloosa, USA
O. Charaf, S.I. Cooper, C. Henderson, P. Rumerio

Boston University, Boston, USA
D. Arcaro, A. Avetisyan, T. Bose, C. Fantasia, D. Gastler, P. Lawson, D. Rankin, C. Richardson, J. Rohlf, J. St. John, L. Sulak, D. Zou

Brown University, Providence, USA
J. Alimena, E. Berry, S. Bhattacharya, D. Cutts, N. Dhingra, A. Ferapontov, A. Garabedian, J. Hakala, U. Heintz, E. Laird, G. Landsberg, Z. Mao, M. Narain, S. Piperov, S. Sagir, R. Syarif

University of California, Davis, Davis, USA
R. Breedon, G. Breto, M. Calderon De La Barca Sanchez, S. Chauhan, M. Chertok, J. Conway, R. Conway, P.T. Cox, R. Erbacher, M. Gardner, W. Ko, R. Lander, M. Mulhearn, D. Pellett, J. Pilot, F. Ricci-Tam, S. Shalhout, J. Smith, M. Squires, D. Stolp, M. Tripathi, S. Wilbur, R. Yohay

University of California, Los Angeles, USA
C. Bravo, R. Cousins, P. Everaerts, C. Farrell, A. Florent, J. Hauser, M. Ignatenko, D. Saltzberg, E. Takasugi, V. Valuev, M. Weber

University of California, Riverside, Riverside, USA
K. Burt, R. Clare, J. Ellison, J.W. Gary, G. Hanson, J. Heilman, M. Ivova PANEVA, P. Jandir, E. Kennedy, F. Lacroix, O.R. Long, A. Luthra, M. Malberti, M. Olmedo Negrete, A. Shrinivas, H. Wei, S. Wimpenny, B. R. Yates

University of California, San Diego, La Jolla, USA
J.G. Branson, G.B. Cerati, S. Cittolin, R.T. D'Agnolo, M. Derdzinski, A. Holzner, R. Kelley, D. Klein, J. Letts, I. Macneill, D. Olivito, S. Padhi, M. Pieri, M. Sani, V. Sharma, S. Simon, M. Tadel, A. Vartak, S. Wasserbaech[63], C. Welke, F. Würthwein, A. Yagil, G. Zevi Della Porta

University of California, Santa Barbara, Santa Barbara, USA
J. Bradmiller-Feld, C. Campagnari, A. Dishaw, V. Dutta, K. Flowers, M. Franco Sevilla, P. Geffert, C. George, F. Golf, L. Gouskos, J. Gran, J. Incandela, N. Mccoll, S.D. Mullin, J. Richman, D. Stuart, I. Suarez, C. West, J. Yoo

California Institute of Technology, Pasadena, USA
D. Anderson, A. Apresyan, A. Bornheim, J. Bunn, Y. Chen, J. Duarte, A. Mott, H.B. Newman, C. Pena, M. Pierini, M. Spiropulu, J.R. Vlimant, S. Xie, R.Y. Zhu

Carnegie Mellon University, Pittsburgh, USA
M.B. Andrews, V. Azzolini, A. Calamba, B. Carlson, T. Ferguson, M. Paulini, J. Russ, M. Sun, H. Vogel, I. Vorobiev

University of Colorado Boulder, Boulder, USA
J.P. Cumalat, W.T. Ford, A. Gaz, F. Jensen, A. Johnson, M. Krohn, T. Mulholland, U. Nauenberg, K. Stenson, S.R. Wagner

Cornell University, Ithaca, USA
J. Alexander, A. Chatterjee, J. Chaves, J. Chu, S. Dittmer, N. Eggert, N. Mirman, G. Nicolas Kaufman, J.R. Patterson, A. Rinkevicius, A. Ryd, L. Skinnari, L. Soffi, W. Sun, S.M. Tan, W.D. Teo, J. Thom, J. Thompson, J. Tucker, Y. Weng, P. Wittich

Fermi National Accelerator Laboratory, Batavia, USA
S. Abdullin, M. Albrow, G. Apollinari, S. Banerjee, L.A.T. Bauerdick, A. Beretvas, J. Berryhill, P.C. Bhat, G. Bolla, K. Burkett, J.N. Butler, H.W.K. Cheung, F. Chlebana, S. Cihangir, V.D. Elvira, I. Fisk, J. Freeman, E. Gottschalk, L. Gray, D. Green, S. Grünendahl, O. Gutsche, J. Hanlon, D. Hare, R.M. Harris, S. Hasegawa, J. Hirschauer, Z. Hu, B. Jayatilaka, S. Jindariani, M. Johnson, U. Joshi, A.W. Jung, B. Klima, B. Kreis, S. Lammel, J. Linacre, D. Lincoln, R. Lipton, T. Liu, R. Lopes De Sá, J. Lykken, K. Maeshima, J.M. Marraffino, V.I. Martinez Outschoorn, S. Maruyama, D. Mason, P. McBride, P. Merkel, K. Mishra, S. Mrenna, S. Nahn, C. Newman-Holmes, V. O'Dell, K. Pedro, O. Prokofyev, G. Rakness, E. Sexton-Kennedy,

A. Soha, W.J. Spalding, L. Spiegel, N. Strobbe, L. Taylor, S. Tkaczyk, N.V. Tran, L. Uplegger, E.W. Vaandering, C. Vernieri, M. Verzocchi, R. Vidal, H.A. Weber, A. Whitbeck

University of Florida, Gainesville, USA
D. Acosta, P. Avery, P. Bortignon, D. Bourilkov, A. Carnes, M. Carver, D. Curry, S. Das, R.D. Field, I.K. Furic, S.V. Gleyzer, J. Hugon, J. Konigsberg, A. Korytov, J.F. Low, P. Ma, K. Matchev, H. Mei, P. Milenovic[64], G. Mitselmakher, D. Rank, R. Rossin, L. Shchutska, M. Snowball, D. Sperka, N. Terentyev, L. Thomas, J. Wang, S. Wang, J. Yelton

Florida International University, Miami, USA
S. Hewamanage, S. Linn, P. Markowitz, G. Martinez, J.L. Rodriguez

Florida State University, Tallahassee, USA
A. Ackert, J.R. Adams, T. Adams, A. Askew, S. Bein, J. Bochenek, B. Diamond, J. Haas, S. Hagopian, V. Hagopian, K.F. Johnson, A. Khatiwada, H. Prosper, M. Weinberg

Florida Institute of Technology, Melbourne, USA
M.M. Baarmand, V. Bhopatkar, S. Colafranceschi[65], M. Hohlmann, H. Kalakhety, D. Noonan, T. Roy, F. Yumiceva

University of Illinois at Chicago (UIC), Chicago, USA
M.R. Adams, L. Apanasevich, D. Berry, R.R. Betts, I. Bucinskaite, R. Cavanaugh, O. Evdokimov, L. Gauthier, C.E. Gerber, D.J. Hofman, P. Kurt, C. O'Brien, I.D. Sandoval Gonzalez, C. Silkworth, P. Turner, N. Varelas, Z. Wu, M. Zakaria

The University of Iowa, Iowa City, USA
B. Bilki[66], W. Clarida, K. Dilsiz, S. Durgut, R.P. Gandrajula, M. Haytmyradov, V. Khristenko, J.-P. Merlo, H. Mermerkaya[67], A. Mestvirishvili, A. Moeller, J. Nachtman, H. Ogul, Y. Onel, F. Ozok[57], A. Penzo, C. Snyder, E. Tiras, J. Wetzel, K. Yi

Johns Hopkins University, Baltimore, USA
I. Anderson, B.A. Barnett, B. Blumenfeld, N. Eminizer, D. Fehling, L. Feng, A.V. Gritsan, P. Maksimovic, C. Martin, M. Osherson, J. Roskes, A. Sady, U. Sarica, M. Swartz, M. Xiao, Y. Xin, C. You

The University of Kansas, Lawrence, USA
P. Baringer, A. Bean, G. Benelli, C. Bruner, R.P. Kenny III, D. Majumder, M. Malek, M. Murray, S. Sanders, R. Stringer, Q. Wang

Kansas State University, Manhattan, USA
A. Ivanov, K. Kaadze, S. Khalil, M. Makouski, Y. Maravin, A. Mohammadi, L.K. Saini, N. Skhirtladze, S. Toda

Lawrence Livermore National Laboratory, Livermore, USA
D. Lange, F. Rebassoo, D. Wright

University of Maryland, College Park, USA
C. Anelli, A. Baden, O. Baron, A. Belloni, B. Calvert, S.C. Eno, C. Ferraioli, J.A. Gomez, N.J. Hadley, S. Jabeen, R.G. Kellogg, T. Kolberg, J. Kunkle, Y. Lu, A.C. Mignerey, Y.H. Shin, A. Skuja, M.B. Tonjes, S.C. Tonwar

Massachusetts Institute of Technology, Cambridge, USA
A. Apyan, R. Barbieri, A. Baty, K. Bierwagen, S. Brandt, W. Busza, I.A. Cali, Z. Demiragli, L. Di Matteo, G. Gomez Ceballos, M. Goncharov, D. Gulhan, Y. Iiyama, G.M. Innocenti, M. Klute, D. Kovalskyi, Y.S. Lai, Y.-J. Lee, A. Levin, P.D. Luckey, A.C. Marini, C. Mcginn,

C. Mironov, S. Narayanan, X. Niu, C. Paus, D. Ralph, C. Roland, G. Roland, J. Salfeld-Nebgen, G.S.F. Stephans, K. Sumorok, M. Varma, D. Velicanu, J. Veverka, J. Wang, T.W. Wang, B. Wyslouch, M. Yang, V. Zhukova

University of Minnesota, Minneapolis, USA
B. Dahmes, A. Evans, A. Finkel, A. Gude, P. Hansen, S. Kalafut, S.C. Kao, K. Klapoetke, Y. Kubota, Z. Lesko, J. Mans, S. Nourbakhsh, N. Ruckstuhl, R. Rusack, N. Tambe, J. Turkewitz

University of Mississippi, Oxford, USA
J.G. Acosta, S. Oliveros

University of Nebraska-Lincoln, Lincoln, USA
E. Avdeeva, K. Bloom, S. Bose, D.R. Claes, A. Dominguez, C. Fangmeier, R. Gonzalez Suarez, R. Kamalieddin, J. Keller, D. Knowlton, I. Kravchenko, F. Meier, J. Monroy, F. Ratnikov, J.E. Siado, G.R. Snow

State University of New York at Buffalo, Buffalo, USA
M. Alyari, J. Dolen, J. George, A. Godshalk, C. Harrington, I. Iashvili, J. Kaisen, A. Kharchilava, A. Kumar, S. Rappoccio, B. Roozbahani

Northeastern University, Boston, USA
G. Alverson, E. Barberis, D. Baumgartel, M. Chasco, A. Hortiangtham, A. Massironi, D.M. Morse, D. Nash, T. Orimoto, R. Teixeira De Lima, D. Trocino, R.-J. Wang, D. Wood, J. Zhang

Northwestern University, Evanston, USA
K.A. Hahn, A. Kubik, N. Mucia, N. Odell, B. Pollack, A. Pozdnyakov, M. Schmitt, S. Stoynev, K. Sung, M. Trovato, M. Velasco

University of Notre Dame, Notre Dame, USA
A. Brinkerhoff, N. Dev, M. Hildreth, C. Jessop, D.J. Karmgard, N. Kellams, K. Lannon, N. Marinelli, F. Meng, C. Mueller, Y. Musienko[37], M. Planer, A. Reinsvold, R. Ruchti, G. Smith, S. Taroni, N. Valls, M. Wayne, M. Wolf, A. Woodard

The Ohio State University, Columbus, USA
L. Antonelli, J. Brinson, B. Bylsma, L.S. Durkin, S. Flowers, A. Hart, C. Hill, R. Hughes, W. Ji, K. Kotov, T.Y. Ling, B. Liu, W. Luo, D. Puigh, M. Rodenburg, B.L. Winer, H.W. Wulsin

Princeton University, Princeton, USA
O. Driga, P. Elmer, J. Hardenbrook, P. Hebda, S.A. Koay, P. Lujan, D. Marlow, T. Medvedeva, M. Mooney, J. Olsen, C. Palmer, P. Piroué, H. Saka, D. Stickland, C. Tully, A. Zuranski

University of Puerto Rico, Mayaguez, USA
S. Malik

Purdue University, West Lafayette, USA
V.E. Barnes, D. Benedetti, D. Bortoletto, L. Gutay, M.K. Jha, M. Jones, K. Jung, D.H. Miller, N. Neumeister, B.C. Radburn-Smith, X. Shi, I. Shipsey, D. Silvers, J. Sun, A. Svyatkovskiy, F. Wang, W. Xie, L. Xu

Purdue University Calumet, Hammond, USA
N. Parashar, J. Stupak

Rice University, Houston, USA
A. Adair, B. Akgun, Z. Chen, K.M. Ecklund, F.J.M. Geurts, M. Guilbaud, W. Li, B. Michlin, M. Northup, B.P. Padley, R. Redjimi, J. Roberts, J. Rorie, Z. Tu, J. Zabel

University of Rochester, Rochester, USA
B. Betchart, A. Bodek, P. de Barbaro, R. Demina, Y. Eshaq, T. Ferbel, M. Galanti, A. Garcia-Bellido, J. Han, A. Harel, O. Hindrichs, A. Khukhunaishvili, G. Petrillo, P. Tan, M. Verzetti

Rutgers, The State University of New Jersey, Piscataway, USA
S. Arora, A. Barker, J.P. Chou, C. Contreras-Campana, E. Contreras-Campana, D. Ferencek, Y. Gershtein, R. Gray, E. Halkiadakis, D. Hidas, E. Hughes, S. Kaplan, R. Kunnawalkam Elayavalli, A. Lath, K. Nash, S. Panwalkar, M. Park, S. Salur, S. Schnetzer, D. Sheffield, S. Somalwar, R. Stone, S. Thomas, P. Thomassen, M. Walker

University of Tennessee, Knoxville, USA
M. Foerster, G. Riley, K. Rose, S. Spanier, A. York

Texas A&M University, College Station, USA
O. Bouhali[68], A. Castaneda Hernandez[68], A. Celik, M. Dalchenko, M. De Mattia, A. Delgado, S. Dildick, R. Eusebi, J. Gilmore, T. Huang, T. Kamon[69], V. Krutelyov, R. Mueller, I. Osipenkov, Y. Pakhotin, R. Patel, A. Perloff, A. Rose, A. Safonov, A. Tatarinov, K.A. Ulmer[2]

Texas Tech University, Lubbock, USA
N. Akchurin, C. Cowden, J. Damgov, C. Dragoiu, P.R. Dudero, J. Faulkner, S. Kunori, K. Lamichhane, S.W. Lee, T. Libeiro, S. Undleeb, I. Volobouev

Vanderbilt University, Nashville, USA
E. Appelt, A.G. Delannoy, S. Greene, A. Gurrola, R. Janjam, W. Johns, C. Maguire, Y. Mao, A. Melo, H. Ni, P. Sheldon, B. Snook, S. Tuo, J. Velkovska, Q. Xu

University of Virginia, Charlottesville, USA
M.W. Arenton, B. Cox, B. Francis, J. Goodell, R. Hirosky, A. Ledovskoy, H. Li, C. Lin, C. Neu, T. Sinthuprasith, X. Sun, Y. Wang, E. Wolfe, J. Wood, F. Xia

Wayne State University, Detroit, USA
C. Clarke, R. Harr, P.E. Karchin, C. Kottachchi Kankanamge Don, P. Lamichhane, J. Sturdy

University of Wisconsin - Madison, Madison, WI, USA
D.A. Belknap, D. Carlsmith, M. Cepeda, S. Dasu, L. Dodd, S. Duric, B. Gomber, M. Grothe, R. Hall-Wilton, M. Herndon, A. Hervé, P. Klabbers, A. Lanaro, A. Levine, K. Long, R. Loveless, A. Mohapatra, I. Ojalvo, T. Perry, G.A. Pierro, G. Polese, T. Ruggles, T. Sarangi, A. Savin, A. Sharma, N. Smith, W.H. Smith, D. Taylor, N. Woods

†: Deceased
1: Also at Vienna University of Technology, Vienna, Austria
2: Also at CERN, European Organization for Nuclear Research, Geneva, Switzerland
3: Also at State Key Laboratory of Nuclear Physics and Technology, Peking University, Beijing, China
4: Also at Institut Pluridisciplinaire Hubert Curien, Université de Strasbourg, Université de Haute Alsace Mulhouse, CNRS/IN2P3, Strasbourg, France
5: Also at National Institute of Chemical Physics and Biophysics, Tallinn, Estonia
6: Also at Skobeltsyn Institute of Nuclear Physics, Lomonosov Moscow State University, Moscow, Russia
7: Also at Universidade Estadual de Campinas, Campinas, Brazil
8: Also at Centre National de la Recherche Scientifique (CNRS) - IN2P3, Paris, France
9: Also at Laboratoire Leprince-Ringuet, Ecole Polytechnique, IN2P3-CNRS, Palaiseau, France
10: Also at Joint Institute for Nuclear Research, Dubna, Russia
11: Now at Suez University, Suez, Egypt

12: Now at British University in Egypt, Cairo, Egypt
13: Also at Cairo University, Cairo, Egypt
14: Also at Fayoum University, El-Fayoum, Egypt
15: Also at Université de Haute Alsace, Mulhouse, France
16: Also at Tbilisi State University, Tbilisi, Georgia
17: Also at RWTH Aachen University, III. Physikalisches Institut A, Aachen, Germany
18: Also at Indian Institute of Science Education and Research, Bhopal, India
19: Also at University of Hamburg, Hamburg, Germany
20: Also at Brandenburg University of Technology, Cottbus, Germany
21: Also at Institute of Nuclear Research ATOMKI, Debrecen, Hungary
22: Also at Eötvös Loránd University, Budapest, Hungary
23: Also at University of Debrecen, Debrecen, Hungary
24: Also at Wigner Research Centre for Physics, Budapest, Hungary
25: Also at University of Visva-Bharati, Santiniketan, India
26: Now at King Abdulaziz University, Jeddah, Saudi Arabia
27: Also at University of Ruhuna, Matara, Sri Lanka
28: Also at Isfahan University of Technology, Isfahan, Iran
29: Also at University of Tehran, Department of Engineering Science, Tehran, Iran
30: Also at Plasma Physics Research Center, Science and Research Branch, Islamic Azad University, Tehran, Iran
31: Also at Università degli Studi di Siena, Siena, Italy
32: Also at Purdue University, West Lafayette, USA
33: Also at International Islamic University of Malaysia, Kuala Lumpur, Malaysia
34: Also at Malaysian Nuclear Agency, MOSTI, Kajang, Malaysia
35: Also at Consejo Nacional de Ciencia y Tecnología, Mexico city, Mexico
36: Also at Warsaw University of Technology, Institute of Electronic Systems, Warsaw, Poland
37: Also at Institute for Nuclear Research, Moscow, Russia
38: Now at National Research Nuclear University 'Moscow Engineering Physics Institute' (MEPhI), Moscow, Russia
39: Also at St. Petersburg State Polytechnical University, St. Petersburg, Russia
40: Also at California Institute of Technology, Pasadena, USA
41: Also at Faculty of Physics, University of Belgrade, Belgrade, Serbia
42: Also at INFN Sezione di Roma; Università di Roma, Roma, Italy
43: Also at National Technical University of Athens, Athens, Greece
44: Also at Scuola Normale e Sezione dell'INFN, Pisa, Italy
45: Also at University of Athens, Athens, Greece
46: Also at Institute for Theoretical and Experimental Physics, Moscow, Russia
47: Also at Albert Einstein Center for Fundamental Physics, Bern, Switzerland
48: Also at Adiyaman University, Adiyaman, Turkey
49: Also at Mersin University, Mersin, Turkey
50: Also at Cag University, Mersin, Turkey
51: Also at Piri Reis University, Istanbul, Turkey
52: Also at Gaziosmanpasa University, Tokat, Turkey
53: Also at Ozyegin University, Istanbul, Turkey
54: Also at Izmir Institute of Technology, Izmir, Turkey
55: Also at Marmara University, Istanbul, Turkey
56: Also at Kafkas University, Kars, Turkey
57: Also at Mimar Sinan University, Istanbul, Istanbul, Turkey
58: Also at Yildiz Technical University, Istanbul, Turkey

59: Also at Hacettepe University, Ankara, Turkey
60: Also at Rutherford Appleton Laboratory, Didcot, United Kingdom
61: Also at School of Physics and Astronomy, University of Southampton, Southampton, United Kingdom
62: Also at Instituto de Astrofísica de Canarias, La Laguna, Spain
63: Also at Utah Valley University, Orem, USA
64: Also at University of Belgrade, Faculty of Physics and Vinca Institute of Nuclear Sciences, Belgrade, Serbia
65: Also at Facoltà Ingegneria, Università di Roma, Roma, Italy
66: Also at Argonne National Laboratory, Argonne, USA
67: Also at Erzincan University, Erzincan, Turkey
68: Also at Texas A&M University at Qatar, Doha, Qatar
69: Also at Kyungpook National University, Daegu, Korea